Heterogeneous dynamics in liquids: fluctuations in space and time

2002 J. Phys.: Condens. Matter 14 R703

(http://iopscience.iop.org/0953-8984/14/23/201)

INSTITUTE OF PHYSICS PUBLISHING JOURNAL OF PHYSICS: CONDENSED MATTER

J. Phys.: Condens. Matter **14** (2002) R703–R738 PII: S0953-8984(02)26721-1

TOPICAL REVIEW

Heterogeneous dynamics in liquids: fluctuations in space and time

Ranko Richert

Department of Chemistry and Biochemistry, Arizona State University, Tempe, AZ 85287-1604, USA

Received 15 January 2002
Published 30 May 2002
Online at stacks.iop.org/JPhysCM/14/R703

Abstract

The disordered nature of glass-forming melts gives rise to non-Arrhenius and non-exponential behaviour of their dynamics. With respect to the microscopic details involved in the structural relaxation, these materials have remained an unsolved puzzle for over a century. The observation of spatial heterogeneity regarding the dynamics provides an important step towards understanding the relation between the macroscopic properties of soft condensed matter and the molecular mechanisms involved. On the other hand, dynamic heterogeneity is the source of several new questions: What is the length scale and persistence time associated with such clusters of relaxation time? What is the signature of heterogeneity at high temperatures and in the glassy state? How do these features depend on the particular material and on the correlation function used for probing these heterogeneities? This work attempts to review the various approaches to heterogeneous dynamics and the generally accepted results, as well as some controversial issues. Undoubtedly, heterogeneity has provoked a number of novel experimental techniques targeted at studying glass-forming liquids at the molecular level. It will be emphasized that the picture of heterogeneity is a requirement for rationalizing an increasing number of experimental observations rather than just an alternative model for the dynamics of molecules.

Contents

0953-8984/02/230703+36$30.00

1. Introduction

Structurally disordered condensed matter is encountered in a number of chemically and physically very different materials, many of which are related to important technical applications [1]. Examples are inorganic glasses, polymeric solids and melts, normal and supercooled liquids, plastic crystals and metallic glasses. X-ray diffraction patterns of such amorphous systems reveal short range order which is reminiscent of the crystalline counterpart, but any longer range order or symmetry remains absent [2]. Accordingly, the intermolecular distances and mutual orientations vary from site to site, leading to a distribution of energy barriers for structural reorganization. A well defined and site-invariant transition rate, the prerequisite for simple dynamics, will therefore remain absent in soft condensed matter and it comes as no surprise that the behaviour of non-crystalline materials is governed by distributed rather than single-valued quantities. The most prominent features resulting from structural disorder are non-exponential relaxation patterns and a non-Arrhenius temperature dependence of some characteristic timescale [3, 4].

The experimental techniques applied in order to observe responses related to structural relaxations are numerous [5–9]. Examples are mechanical shear stress measurements, nuclear magnetic resonance techniques, dielectric relaxation, various light scattering and photon correlation spectroscopies, enthalpy or volume recovery after a temperature jump, dynamic heat capacity and thermal expansivity methods, and neutron scattering, to name only a few. The typical protocol is to apply a perturbation at time zero and to measure the gradual approach towards equilibrium as a function of time. For sufficiently small perturbations, i.e. in the regime of linear responses, the fluctuation–dissipation theorem (FDT) states that the resulting shape of the relaxation function is determined solely by the equilibrium fluctuations. The observed quantity and the experimental situation determines which time correlation function is being measured [10]. Although the above examples of relaxation experiments all relate to different correlation functions, the fact that some reorganization of molecular structure is involved in each case leads to the observed universality of non-exponential relaxations in disordered materials, often following the stretched exponential or Kohlrausch–Williams–Watts (KWW) type decay [11, 12],

$$\phi(t) = \phi_0 \exp\left[-\left(\frac{t}{\tau_{KWW}}\right)^{\beta_{KWW}}\right]. \tag{1}$$

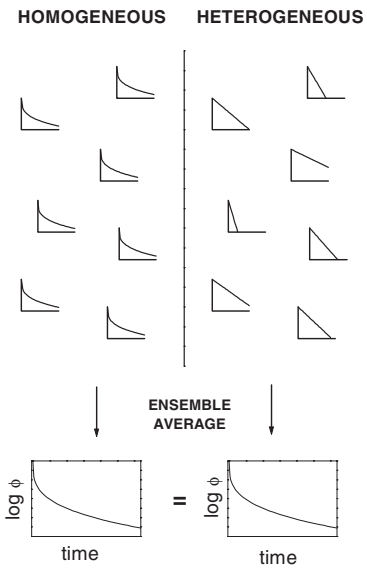

Figure 1. Schematic representation of two different sources of non-exponential correlation decays [13]. The left part outlines a *homogeneous* relaxation scenario, in which all local contributions are identical to the ensemble average. The right side refers to *heterogeneous* dynamics, characterized by individual relaxing units having site specific relaxation times. By virtue of the ensemble average the two distinct relaxation models can lead to the same decay pattern if only the macroscopic response is considered.

In the more general case, any correlation function can be cast into the form of a superposition of exponentials with some appropriate probability density $g(\tau)$ for the relaxation times τ,

$$\phi(t) = \int_0^\infty g(\tau) \mathrm{e}^{-\frac{t}{\tau}} \mathrm{d}\tau = \langle \exp(-t/\tau) \rangle. \tag{2}$$

The deviations from simple exponential patterns seen in practically all relaxation experiments of liquids imply that more than one timescale is required in order to characterize the ensemble-averaged process. At this point, it is easily realized that there are many different ways of introducing a distribution of timescales which all lead to the same relaxation pattern after averaging over the ensemble of relaxing units. Figure 1 confronts two extreme cases out of the many possible dynamical models [13]. In the spatially homogeneous case, each site within the sample contributes identically to the relaxation function, such that local and ensemble-averaged dynamics are the same. In the other extreme, every local relaxation is associated with purely exponential dynamics, combined with a spatial distribution of time constants in order to arrive at non-exponentiality regarding the ensemble average. The former case, dynamic homogeneity, is an attractive model because every site is representative of the macroscopic behaviour, which simplifies matters quite drastically. The alternative picture of dynamical heterogeneity leads to a number of additional questions which will be discussed further below. As long as one is interested in the macroscopic, i.e. ensemble-averaged, quantities only, one could argue that the microscopic details are of little relevance. On the other hand, the two cases outlined in figure 1 are associated with entirely different understandings and theoretical approaches regarding the molecular mechanisms which determine the dynamics. According to the recent advances in this active area of research, understanding the behaviour of soft condensed matter on the molecular scale is considered a prerequisite to rationalizing the macroscopic properties.

The motivation for studying the nature of dispersive relaxation processes in more detail has prompted the search for experimental techniques capable of discriminating between homogeneous and heterogeneous dynamics. An experiment aimed at revealing dynamic heterogeneity needs to supply more information than provided by a macroscopic relaxation trace recorded within the regime of linear responses. The initial approaches to heterogeneous dynamics exploited the possibility to select a dynamical subensemble, for example those units which relax slower than average, and to determine whether they remain slow for some time [14]. Already the observation of such a spectral selectivity justifies concluding on heterogeneous dynamics [15]. Later on, other techniques were devised in order to gain more quantitative insight into the nature of the dynamics in disordered materials. Yet, only a few experimental methods are capable of contributing directly to this fascinating area of research.

The majority of experiments, simulations and models concerned with heterogeneous dynamics focus on the primary or α-relaxation processes in the liquid state, i.e. above the glass transition temperature T_g. This temperature T_g indicates the transition from the equilibrium liquid state to the solid-like glassy state, in which larger scale molecular motion is frozen. In practice, this glass transition is often identified with the temperature at which the viscosity reaches a value of $\eta = 10^{13}$ Poise or where the relaxation time is $\tau = 10^2$ s. Relaxation phenomena occurring in the vitreous state below T_g have also been identified as heterogeneous. The observation of heterogeneity regarding the primary structural relaxation raises many additional questions: Are the different coexisting timescales spatially clustered? What is the response function of an individual relaxing unit, exponential or dispersive? How long does a timescale remain associated with a given site? What are the spatial dimensions of this heterogeneity? How does heterogeneity affect the glassy state below T_g? Of particular interest is whether heterogeneity implies length scales other than the size of cooperatively rearranging regions and timescales other than the structural relaxation time.

2. Dynamics in amorphous materials

A material cooled to below its melting temperature T_m is considered a supercooled liquid if crystallization has not occurred. In this case, discontinuous changes of the material properties remain absent near T_m and the predominant effect of temperature is to vary the viscosity η and in parallel the structural relaxation time τ. In a relatively narrow temperature interval below T_m, both η and τ are often observed to increase by 12 orders of magnitude while the material remains in the equilibrium liquid state. In many cases, this increase in viscosity upon cooling is accompanied by a significant change in the apparent activation energy. A purely empirical relation for describing the temperature dependence of oils above T_m with a small number of parameters has been introduced by Vogel in 1921 [16], which was then discussed in the context of more viscous melts by Fulcher [17] and by Tammann and Hesse [18]. This Vogel–Fulcher–Tammann (VFT) law,

$$\tau(T) = \tau_0 \exp\left[\frac{DT_0}{T - T_0}\right], \tag{3}$$

is still widely used in order to characterize the temperature dependence of transport coefficients in the entire regime of the equilibrium liquid. It is equivalent to the Williams–Landel–Ferry (WLF) relation established for shift factors in polymers [19]. The Arrhenius law is recovered in the limit of a vanishing Vogel temperature T_0 and D is related to the fragility of the material [20]. An important aspect of this VFT relation is the implied divergence of the relaxation time τ at a finite temperature $T_0 > 0$, which has prompted the search for an underlying phase transition [21]. In practice, however, it is the finite cooling rate or

equilibration time that lets every real system enter the non-equilibrium glassy state before the proximity to T_0 becomes an issue.

One of the early attempts to rationalize the VFT relation is the free volume theory, which assumes that a certain amount of local unobstructed volume is required in order for some molecular motion to occur [22,23]. Within this picture, the VFT law is supported if the *ad hoc* assumption is made that the amount of free volume available depends linearly on temperature. A drawback of this approach is its incompatibility with experimental results concerning the pressure dependence of the relaxation time [24]. An alternative route has been advanced by Adam and Gibbs [25] in terms of 'cooperatively rearranging regions' (CRRs), where a link between the temperature-dependent configurational entropy $S_c(T)$ and relaxation time τ has been established,

$$\tau(T) = \tau_0 \exp\left[\frac{c}{T S_c(T)}\right]. \tag{4}$$

The simple temperature dependence $S_c(T) = S_\infty - K/T$ required to arrive at a VFT type $\tau(T)$ is supported by the results of calorimetric experiments [26,27]. Various studies have been devoted to estimating the number of molecules within a CRR and the length scale ξ_C associated with these CRRs. This length scale ξ_C of cooperative motion can be envisioned as the minimum distance of two molecules whose motions are mutually independent. It is not related to the diverging correlation lengths discussed in the context of the glass transition [21,28]. Within this picture, lowering the temperature increases the size ξ_C of the CRRs and thereby the apparent activation energy for structural relaxation. A number of experimental results and models are consistent with a growing length scale of cooperativity upon lowering the temperature and values around $\xi_C \approx 3$ nm at T_g have been reported [29–35].

Many other attempts have been made to explain the observed temperature dependence of some characteristic timescale associated with structural relaxation. Examples are the relation $\tau \propto \exp(B/(T - T_0)^{3/2})$ of Bendler and Shlesinger [36], the $\tau \propto \exp(T_0^2/T^2)$ law suggested by Ferry [37] and reestablished by Bässler and Richert on the basis of transport results obtained for random walks in energetically disordered systems [38, 39], the Souletie scaling $\tau \propto (1 - T_c/T)^{-\gamma}$ [40, 41], the dynamic scaling law $\tau \propto (T - T_c)^{-\gamma}$ with $T_c < T_g$ advanced by Colby using percolation ideas [42] and the idealized mode-coupling theory (MCT) again predicting $\tau \propto (T - T_c)^{-\gamma}$ but with $T_c > T_g$ [43]. Models of $\tau(T)$ explicitly invoking heterogeneity will be discussed further below.

A closer scrutiny of the temperature dependence $\tau(T)$ reveals that a single VFT curve is often insufficient for capturing the full details of the experimental findings [44]. Derivative analyses focusing on the quantities $\partial^n \log \tau(T)/\partial T^n$ indicate a change in the activation parameter $B = DT_0$ in equation (3) at a temperature T_B at which the relaxation time is usually near $\tau_B = 10^{-7}$ s [45,46]. For many materials, this feature in $\tau(T)$ coincides with the critical temperature T_c ($\approx 1.2 \times T_g$) of the mode-coupling theory [47], with the extrapolated merging temperature T_β of a secondary or Johari–Goldstein (JG) [48, 49] β-process with the primary α-process [50], and with the temperature above which the Adam–Gibbs theory fails to reproduce relaxation times on the basis of configurational entropy data [47]. It is also near the temperature for which Goldstein [51] anticipated a crossover into the landscape-dominated regime upon cooling. Schönhals has suggested a method for identifying this crossover temperature using a $\Delta\varepsilon$ versus $\log(f_{\max})$ plot based on dielectric data [52]. At a higher temperature T_A, characterized by a relaxation time of $\tau_A \approx 10^{-10}$ s, a further crossover to pure Arrhenius behaviour can be observed [53]. Although such breakpoints in $\tau(T)$ are helpful in finding common patterns in the dynamics of liquids, they should not encourage us to seek models which apply in certain temperature intervals only. Instead, these features are expected to emerge from a realistic model of liquid dynamics without further assumptions.

The above discussion of the temperature dependence of the relaxation timescale τ has disregarded that practically all disordered systems exhibit a dispersion of relaxation times. Often enough, this distribution of time constants is observed in terms of a non-exponential correlation function which is well described by a KWW or stretched exponential function given in equation (1) [54]. Apart from deviations at short times, KWW type decays appear to be a universal behaviour of relaxations in disordered matter. Models in support of the stretched exponential law are the hierarchical picture by Palmer *et al* [55] and Ngai's coupling scheme [56–58]. Further common functions associated with non-exponential responses are the Cole–Cole ($\gamma = 1$), Cole–Davidson ($\alpha = 1$) and Havriliak–Negami ($0 < \alpha, \alpha\gamma \leqslant 1$) expressions

$$\varepsilon^*(\omega) = \varepsilon_\infty + \frac{\varepsilon_s - \varepsilon_\infty}{[1 + (\mathrm{i}\omega\tau)^\alpha]^\gamma}, \tag{5}$$

which are most commonly applied in the context of frequency domain dielectric relaxation data [59]. More recent approaches to non-exponential correlation functions involve the application of fractional calculus and result in equations which are non-local in time [60,61]. A particular case studied by Hilfer [62,63] replicates the Cole–Cole function, which corresponds to a symmetric loss peak on the $\log(\omega)$ scale.

Near T_g, relaxation time dispersions covering several orders of magnitude are the rule for supercooled liquids and polymeric materials. Towards higher temperatures, the widths of these distributions tend to decrease in molecular liquids, whereas temperature-invariant dispersions are seen more often in the case of polymers [64]. The situation of time–temperature superposition or thermorheologic simplicity is a consequence of a constant shape of the correlation function, equivalent to the observation that the only effect of temperature is to shift the average relaxation time while leaving the dispersion unaltered. For a series of molecular liquids investigated by Olsen *et al*, it turns out that the validity of time–temperature superposition near T_g coincides with a certain value of the stretching exponent, $\beta_{KWW} = 0.5$ [65]. In light of these broad distributions of relaxation time constants, the question arises of which timescale is preferred for delineating the temperature dependence in the absence of time–temperature superposition. In general, the $\tau(T)$ curve will depend on whether τ is defined as the peak value, the average or some other characteristic point within the distribution. On the other hand, the shape of the distribution is a rather mild function of temperature compared with how its average value shifts with temperature. Although the particular choice of the characteristic timescale is somewhat arbitrary, it usually has little effect on the overall shape of the $\tau(T)$ curve [45].

The two deviations from simple behaviour discussed above, the non-Arrhenius and non-exponential character of liquid dynamics, are entangled quantities. Both parameters vary systematically along the strong–fragile pattern of glass-forming materials, which gauges the change in the apparent activation energy in the entire range between phonon frequencies and the glass transition, i.e. 10^{-14} s $\leqslant \tau \leqslant 10^2$ s [20]. Fragility can be quantified in different ways: the strength index D as in equation (3), the fragility index m given by [66]

$$m = \left.\frac{\mathrm{d}\log_{10}\langle\tau/s\rangle}{\mathrm{d}(T_g/T)}\right|_{T=T_g} \tag{6}$$

and the fragility in terms of $F_{1/2} = 2T_g/T_{1/2} - 1$ with $\tau(T_{1/2}) = 10^{-6}$ s [47]. Böhmer *et al* have observed for approximately 70 glass-formers that the stretching exponent β_{KWW} increases as the fragility index decreases [66, 67]. Accordingly, the extents to which a system deviates from Arrhenius and from exponential behaviour are correlated. This underlines the importance of understanding the origin of non-exponential correlation functions in soft condensed matter on a molecular level.

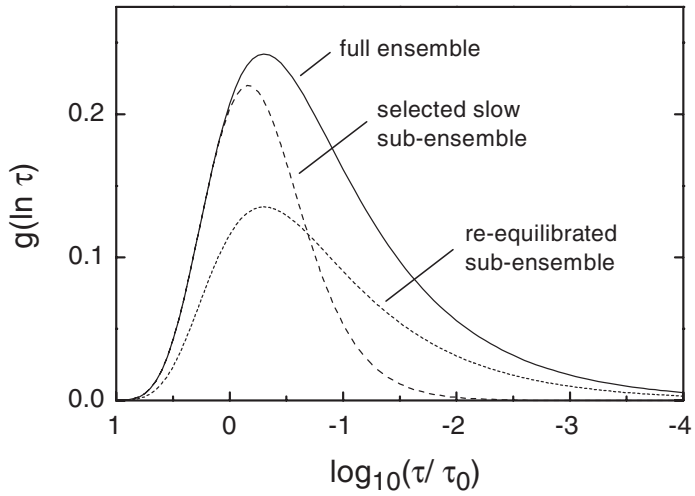

Figure 2. Schematic outline of the concept of spectral filtering in terms of the probability density $g(\ln \tau)$ of relaxation times τ. The solid curve represents the full (unfiltered) ensemble. The dashed curve refers to the situation directly after applying a low pass spectral filter, resulting in a slower and more exponential distribution. In the long time limit shown as a dotted curve, the selected slow subensemble will regain the shape of the full ensemble via rate exchange, while retaining the area of the filtered subensemble.

3. Approaches to heterogeneity

The aim of this section is to provide an overview over the different techniques used to approach heterogeneous dynamics. Again, it is important to realize that heterogeneity is being observed in chemically homogeneous systems with no obvious spatial variation of structure or density. Each method discussed below is associated with its particular range of accessible time and temperature scales, restriction regarding material selection and strength in contributing to one or more of the aspects of heterogeneity in a quantitative fashion. Because not all the details can be discussed here, the reader is referred to the original papers in order to fully appreciate the results. Previous reviews on experimental [68–71] and theoretical [72] work on heterogeneous dynamics are also excellent sources of additional information.

The observation of a two-time correlation function alone is insufficient for discriminating between homogeneous and heterogeneous dynamics if the experiment is conducted within the regime of linear responses. The shape of a relaxation function can be modified by selecting perturbation profiles other than the usual pulse or step method. Within the linear regime, however, emphasizing slow or fast contributions in this manner is not related to spectral selectivity, it is rather a direct consequence of the superposition principle or causality, which holds whenever the amplitudes of response and perturbation are proportional quantities [73,74].

The techniques of nuclear magnetic resonance and photobleaching, as well as dielectric and magnetic hole burning, have in common that a dynamical subensemble, i.e. those sites associated with a subset of relaxation times, is modified or observed selectively. The concept of spectral selectivity regarding the distribution of relaxation times and its return to equilibrium is outlined schematically in figure 2. Occasionally, these methods are referred to as 'hole burning' experiments, in analogy to the optical hole burning performed in low temperature glasses. Optical hole burning exploits the possibility of modifying an extremely narrow subset of transition frequencies (those which are in resonance with the laser frequency) out of the entire inhomogeneously broadened absorption spectrum of chromophores in a relatively

rigid matrix [75–77]. These studies demonstrate clearly that the inhomogeneous broadening of optical lines originates from the previously anticipated heterogeneity regarding the local electric fields [78]. This spectral heterogeneity has been related to functional heterogeneities in biological molecules [79], but there is no direct relation to the heterogeneity of relaxation times regarding structural dynamics.

3.1. Nuclear magnetic resonance

Various techniques based on nuclear magnetic resonance (NMR) have contributed to the field of heterogeneity. In certain experimental situations, spin–lattice relaxations should be exponential in dynamically homogeneous systems [80]. Therefore, some observations of non-exponential spin magnetization near or below T_g are suggestive of heterogeneity, albeit without quantitative results regarding length scales and lifetimes of the domains [81]. NMR experiments have also played a role in establishing the decoupling of the translational diffusion D_{trans} from the rotational diffusion D_{rot}. The relation of this translation–rotation decoupling to heterogeneous dynamics is discussed further in section 3.5 below.

The initial and most important results concerning heterogeneity which have been derived from NMR methods are based upon multi-dimensional (four- or reduced four-dimensional) NMR techniques. Schmidt–Rohr and Spiess have used a reduced four-dimensional NMR method in order to assess higher order time correlation functions of molecular orientations [14]. The first two times constitute a spectral filter, which eliminates all spins which have reoriented a certain amount in a predetermined time interval. Therefore, the remaining spins are associated with slower than average orientation correlation times within the time interval of the filter. A two-time correlation experiment of this spectrally selected subset of slow contributions is already sufficient to demonstrate heterogeneity, because the subset has relaxed slower than the entire ensemble. The next level of sophistication in this experiment is to subject the subset created by the first filter to a further low pass filter after an adjustable re-equilibration period t_{re}. In cases of small t_{re} the second filter will not reduce the signal significantly, but with increasing re-equilibration time the initially selected slow modes will re-equilibrate to become faster ones and thereby not pass the second filter [82]. Such an experiment reveals the persistence time of particular relaxation rates, which is often referred to as rate memory or rate exchange [83]. Based on a statistical analysis, Heuer has given a clear definition of rate exchange in terms of a single rate memory parameter Q, which reflects the fluctuations within the heterogeneous distribution of relaxation rates [84]. These fluctuations represent an important aspect of heterogeneous dynamics.

With this multi-dimensional NMR technique, the observation of spectral selectivity alone (at small t_{re}) is considered proof for the coexistence of slow and fast modes, i.e. of heterogeneity regarding the dynamics [15]. By varying the re-equilibration time t_{re}, this method is then capable of assessing the timescale on which the selected slow subset of reorientation times redistributes into the full set of relaxation times [83, 85–87]. The angular jump correlation function for a selected slower subensemble is compared with the full ensemble in figure 3, based on multi-dimensional NMR results on *ortho*-terphenyl reported by Böhmer *et al* [86]. In this experiment, the angular jump correlation function of the selected subset of spins is clearly slower and more exponential than the unfiltered counterpart.

The multi-dimensional NMR experiments mentioned above do not specify whether similar or identical relaxation times are spatially clustered. A spatial component can be introduced by exploiting the effects of spin diffusion in real space as an additional feature within the multi-dimensional NMR experiment [88,89]. After selecting the slowly reorienting molecules, spins are transferred from ^{13}C to ^{1}H nuclei by cross polarization in order to promote spin diffusion.

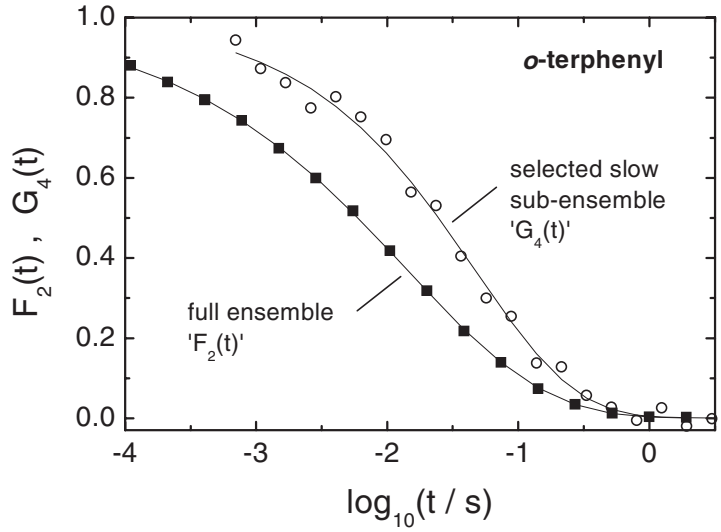

Figure 3. Angular jump correlation function from multi-dimensional NMR experiments on *ortho*-terphenyl. The curve marked 'F_2' is for the un-filtered or two-time correlation function. The designation 'G_4' refers to the filtered or four-time correlation function. Clearly, the selected subset relaxes more slowly and exponentially than does the full ensemble. Adapted with permission from figure 3 of [86].

The diffusion process is interrupted by a $^1\mathrm{H} \rightarrow {}^{13}\mathrm{C}$ backtransfer, and the signal after a second low pass filter is used to quantify the amount of spins still associated with slowly relaxing regions. By varying the extent of spin diffusion, it is then possible to estimate the cluster size of the heterogeneity.

Details of the multi-dimensional NMR techniques and their applications to heterogeneous dynamics in polymers and molecular liquids can be found elsewhere [90–92].

3.2. Deep photobleaching

Cicerone and Ediger [93] have devised an experiment which allows us to record the slow recovery of isotropic probe orientation after inducing optical anisotropy by photochemical bleaching. Probe molecules are dispersed at low concentration in the supercooled liquid under study and irradiated with polarized light for a period of time which is short compared with the timescale of probe reorientation. This photobleaching process removes preferentially those probes from the absorption spectrum whose transition dipole moment for absorption is aligned with the polarization direction of the light source. The observed decay of the resulting optical anisotropy is a direct measure for the single-particle reorientation of the probe molecules.

Spectral selectivity is introduced by a method referred to as deep bleach, where a significant percentage ($>10\%$) of the probe molecules are irreversibly photobleached via peroxidation by exposing the sample to light for a longer period of time [94]. Those probes surviving the deep bleach have been observed to display longer reorientation times compared with the equilibrium distribution before the deep bleach. Several sources for this dynamical selectivity are possible:

(i) slow probes are selectively located in regions of higher density which hinders the conformational changes required for peroxidation;
(ii) slow probes preferentially reside in regions of lower oxygen diffusivity,

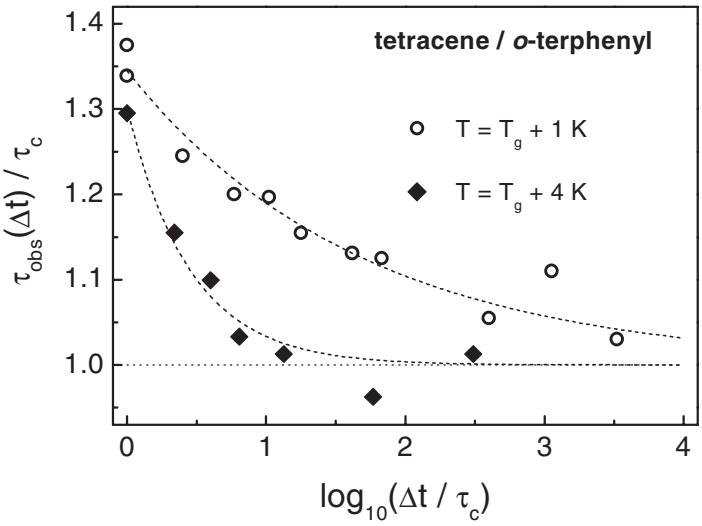

Figure 4. Results of photobleaching experiments on the rotation correlation function of tetracene in *ortho*-terphenyl at two different temperatures relative to $T_g = 243$ K. The deep bleach selects a subset of probes that rotate about 30% slower than the full ensemble. The data demonstrate the time it takes the selected slow subensemble with rotation time $\tau_{obs} \geqslant \tau_c$ to recover to the average relaxation time τ_c of the initial full ensemble. The decays of these curves define the exchange time τ_x. Based on data from [95] and adapted with permission from figure 4(c) of [68].

(iii) probes with transition dipoles oriented persistently along the direction of the incident light beam will not be photobleached.

Any of the three explanations lead to the slowly reorienting probes surviving the bleach process with higher probability. After the deep bleach, the (shallow) photobleach method described above is applied after various waiting times in order to observe how the distorted distribution of reorientation times returns to the original distribution as a function of time. Because probes are required to alter their reorientation time in order for the equilibrium distribution to be re-established, this is a direct measurement of rate exchange effects. With this technique, exchange timescales which are orders of magnitude slower than the average relaxation time have been reported for *ortho*-terphenyl [95] and for polystyrene [96]. Experimental data revealing this very slow return of the selected subensemble to the steady state distribution are shown in figure 4. Here, the signature of spectral selectivity is the initial departure of the average rotation time τ_{obs} of the selected subensemble from the timescale τ_c of the full ensemble. Rate exchange is responsible for τ_{obs} approaching τ_c in the long time limit. For this experiment, probe molecules of appropriate sizes are required in order to assure that the reorientation of the guest molecules tracks the host dynamics. The effects of using larger probes and their relation to heterogeneous dynamics are discussed in section 3.6.

This method is somewhat similar to the NMR approach and the scheme outlined in figure 2. The deep bleach constitutes a spectral filter, and the subsequent dynamics of the selected subset indicates heterogeneity if they are modified compared with the unfiltered ensemble. Probing the distribution of reorientation times after different re-equilibration intervals then reveals directly the time required to reestablish the distribution of the unfiltered ensemble, which is similar to measuring the timescale of rate exchange by varying the re-equilibration period of the multi-dimensional NMR experiment.

3.3. Dielectric and magnetic hole burning

In contrast to multi-dimensional NMR and deep photobleaching, dielectric hole burning (DHB) does not filter or eliminate the contributions of dynamical subsets, but rather alters their response function [97]. The dielectric polarization of disordered materials with dipolar constituents is determined by the response of the macroscopic dipole moment to field- or charge-induced perturbations. Here, the important molecular motion is the reorientation of molecules with permanent dipole moments. Another relevant property of dipolar liquids near their glass transition temperature is that the relaxation amplitude is only moderately sensitive to temperature, while the relaxation time usually displays a pronounced temperature dependence. Time-dependent dielectric polarizations are accompanied by dielectric loss, i.e. by energy being absorbed in the sample whenever time-dependent external fields are being applied. In the DHB technique, a large sinusoidal external electric field is applied and the polarization $\phi^*(t)$ measured after this burn (or pump) process is compared with the situation, $\phi(t)$, without burning. A special measurement protocol is used in order to subtract out the direct linear response to the burn fields [98]. Although other models of DHB effects have been reported [99, 100], an intuitive picture is to make 'heating' in terms of the dissipated energy responsible for changes in the time-dependent polarization. At sufficiently high sinusoidal 'burn' fields, $E_b \sin(\omega_b t)$, the absorbed energy $Q \propto \varepsilon''(\omega_b) E_b^2$ leads to an increase in the fictive temperature, $T_f > T$.

In the case of non-zero difference signals $\Delta\phi(t) = \phi^*(t) - \phi(t)$, the analysis focuses on the question of whether the dielectric response has been modified in a spectrally selective or uniform fashion. In terms of the 'heating' effect, one asks whether a dynamical subset or the entire ensemble has absorbed the energy and thus experienced a change in the fictive temperature. In the former case, only those relaxing units whose response times coincide with the burn frequencies undergo 'heating' and shift towards shorter timescales or higher frequencies. Near the burn frequencies, this leaves a 'hole' in the distribution of relaxation times while creating an 'antihole' in the regime of faster contributions. The effect of such a spectrally selective increase in fictive temperature on the probability density of relaxation times is depicted in figure 5. Note that the $g(\ln\tau)$ curves in figure 5 are not based on experimental evidence. However, it can be shown that such a hole/anti-hole modification of the probability density $g(\tau)$ is compatible with the difference signals $\Delta\phi(t)$ observed in the time domain [101]. A requirement for concluding on heterogeneous dynamics is to observe that the spectral position of the hole shifts upon varying the burn frequency. The 'heating' picture of DHB effects suggests that the extent of modification (hole area or depth) depends quadratically on the burn field amplitude, i.e. linearly on the burn energy. Both features are usually seen in DHB experiments [102].

In most systems it is predominantly the relaxation timescale which changes with temperature instead of the relaxation strength. Therefore, spectrally selective 'heating' shifts part of the probability density $g(\tau)$ of relaxation times τ towards smaller values of τ without significantly affecting the total relaxation strength. Accordingly, a scrutiny of the 'horizontal' difference $\Delta[-\ln(t'/s)](t)$ between $\phi^*(t')$ and $\phi(t')$ is more decisive than is the 'vertical' difference $\Delta\phi(t)$ [97]. For small $\Delta\phi(t)$, this 'horizontal' difference is easily obtained from $\Delta\phi(t)$ by multiplying with the inverse slope of $\phi(t)$ via

$$\Delta[-\ln(t/s)](t) = \Delta\phi(t)\left(\frac{\mathrm{d}\phi(t)}{\mathrm{d}\ln(t/s)}\right)^{-1}. \tag{7}$$

Uniform heating would lead to a time-invariant shift $\Delta\ln(t')$ along the logarithmic time axis, whereas spectrally selective 'heating' results in $\Delta\ln(t') \to 0$ in the limits of short and long times and a maximum whose position is determined by the burn frequency. An example

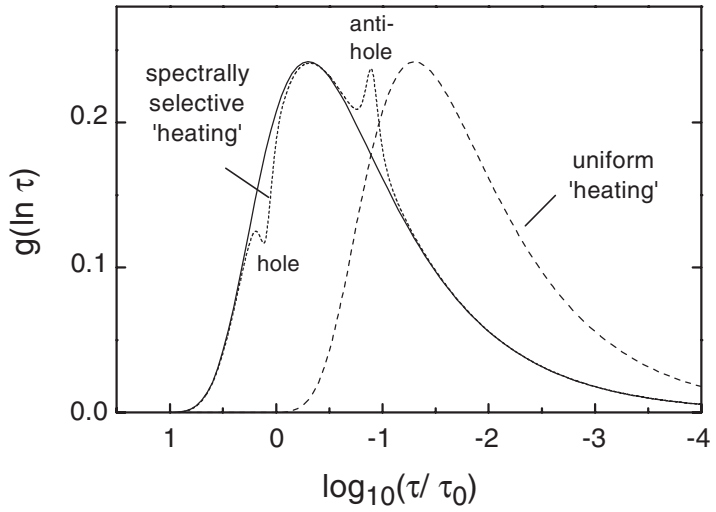

Figure 5. Schematic explanation of the DHB experiment in terms of 'heating' or increase in fictive temperature, $T_f > T$. The solid curve represents the unmodified probability density $g(\ln \tau)$ of relaxation times τ. The dashed curve would result from uniform heating, while the dotted curve outlines $g(\ln \tau)$ as modified by the burn process. Within this picture, hole and anti-hole result from selectively increasing the fictive temperature of a narrow spectral range near $\tau = \tau_0$.

for such a situation is the hole-burning experiment on the Johari–Goldstein β-relaxation in vitreous D-sorbitol, shown as the 'horizontal' difference curve in figure 6. Note that the $\Delta \ln(t')$ signal of figure 6 tends to approach zero for frequencies sufficiently far away from the burn frequency ω_b in either direction, although this behaviour has not been generated by normalization procedures [103].

Two different methods have been applied in order to measure the time-dependent polarization following the burn process: recording the charge flow at constant electric field which yields the dielectric function $\varepsilon(t)$ and recording the voltage change at constant dielectric displacement which refers to the electric modulus $M(t)$. In the frequency domain, the relation between these two quantities is given by $M^*(\omega) = 1/\varepsilon^*(\omega)$. The modulus detection has turned out to be particularly useful for studying vitreous ionic conductors with respect to the heterogeneity of charge carrier diffusivities [104].

Because dielectric hole burning is capable of modifying the response in a spectrally selective fashion, the method has demonstrated heterogeneity of the α-process in molecular glass-formers [98], of the Johari–Goldstein type β-process in vitreous D-sorbitol [103], of the dielectric response of the relaxor ferroelectric system $PbMg_{1/3}Nb_{2/3}O_3$ (PMN) [105] and of the dispersive ion diffusivity in vitreous $2Ca(NO_3)_2{\cdot}3KNO_3$ (CKN) [104]. An additional parameter in this experiment is the waiting time t_w between the burn process and probing the response. In some cases, the burn effect in the response is long lived compared with the timescale of the modified relaxation times [103,105]. In the 'heating' scenario, this persistence time of the 'hole' reflects the time it takes the local fictive temperature to re-equilibrate rather than the timescale of rate exchange. On the other hand, it seems plausible that rate exchange must limit the time a modification of the response can remain spectrally selective. Therefore, the persistence times of spectral holes should establish a lower bound for the timescale of rate exchange.

The magnetic analogue of DHB is magnetic hole burning (MHB), where a large sinusoidal magnetic field is employed in order to modify the time-dependent magnetization.

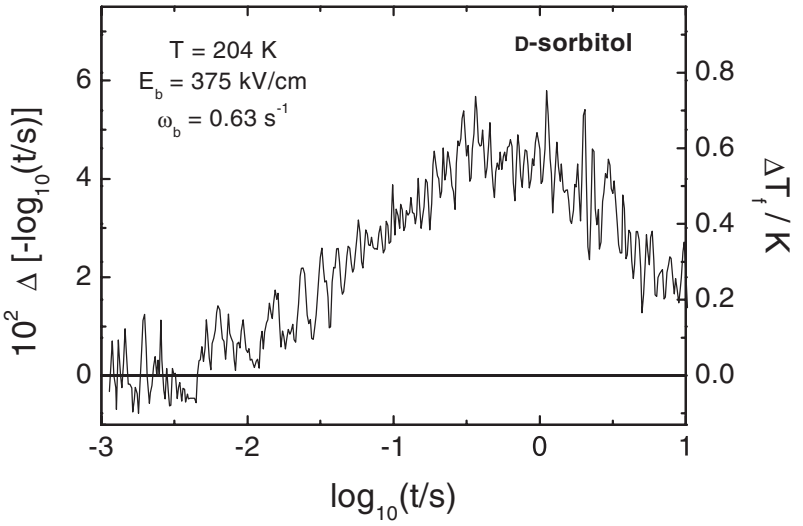

Figure 6. Modulus-detected DHB result for the β-relaxation of a vitreous 8 μm thick sample of D-sorbitol at $T = 204$ K [103]. The burn field and frequency are $E_b = 375$ kV cm^{-1} and $\omega_b = 0.63$ s^{-1}, respectively. The curve refers to the 'horizontal' difference $\Delta[-\log_{10}(t/s)]$ between $M(t)$ and $M^*(t)$. The parameters for the 'vertical' difference $\Delta M(t) = [M(t) - M^*(t)]/M_\infty$ are peak position $\log_{10}(t_{max}/s) = -0.45$, peak amplitude $\Delta M_{max} = \Delta M(t_{max}) = 1.4 \times 10^{-3}$ and an FWHM width of $\approx$1.8 decades. The ΔT_f scale is related to $\Delta[-\log_{10}(t/s)]$ via the Arrhenius activation parameter $B = 3122$ K.

This technique has been applied to a 5% Au:Fe spin glass [106]. The protocol for eliminating the direct linear response parallels essentially that used in the dielectric counterpart. In these MHB experiments, it has been found that the temperature relative to T_g governs whether the dominant hole-burning mechanism is based on a modification of the relaxation times or of the response amplitudes. Therefore, the burn-induced modification often produces a step rather than a peak in the difference signal $\Delta\phi(t) = \phi^*(t) - \phi(t)$. A particularly striking observation in this study is that large amplitude magnetic fields heated parts of the sample above the transition temperature, while other parts remained a spin glass, i.e. below T_g.

As mentioned already, modifying the response function by non-resonant hole-burning techniques relies on driving the system beyond the linear response regime. At sufficiently high fields, one encounters both the effects of saturation (non-linearity regarding the response amplitude) and the effects of dissipated energy ('heating'). A non-linear behaviour of the response amplitude alone can give rise to modifications whose position on the timescale depend on the pump frequency, which have been explained without invoking heterogeneous dynamics [107, 108]. On the other hand, non-linear responses have been considered explicitly within an asymmetric double-well potential (ADWP) model in order to argue that non-resonant hole burning is a decisive method regarding the discrimination of heterogeneous and homogeneous dynamics [99, 100]. Although the 'heating' or increased fictive temperature approach is linear in the dissipated energy, it is also non-linear in the driving field. Irrespective of how the non-linearity of the response is modelled, pump-frequency-dependent modifications alone are insufficient for concluding on heterogeneous dynamics. This is especially true if the signals are subject to normalization procedures which force the difference $\Delta\phi(t)$ to zero at short and long times.

3.4. Solvation dynamics

Emission energies of chromophores are sensitive to the interactions with the solvent molecules. In situations where the solvent structure responds to solute excitation within the lifetime of the excited state, time-dependent emission energies can be observed in solvation dynamics (SD) experiments [109]. If the interactions between permanent dipoles dominate, the effects are referred to as dipolar solvation and the reorientation of solvent molecules is considered the most important mode in shifting the solvation free energy of the probe molecule [110]. An alternative view is to regard solvation dynamics as being a dielectric polarization experiment in the local and inhomogeneous electric field produced by the excited state charge distribution of the probe molecule. Such a measurement is realized by laser pulse excitation of the chromophores which are present at low concentration in a glass-forming solvent and recording the emission spectra as a function of time [111]. Matching the excited state lifetime with the slow structural timescales of viscous liquids near T_g is accomplished using long lived triplet state probes [112, 113].

The time-resolved emission spectra obtained from triplet state SD experiments are well approximated by Gaussian profiles. Their mean energies shift towards lower values with increasing time, thereby indicating that the polarization of the surrounding solvent approaches steady state conditions. This dynamics is often expressed in terms of the Stokes-shift correlation function $C(t)$, i.e. after normalizing the average energies to their limiting values at $t = 0$ and $t \to \infty$,

$$C(t) = \frac{\langle\omega(t)\rangle - \langle\omega(\infty)\rangle}{\langle\omega(0)\rangle - \langle\omega(\infty)\rangle}. \tag{8}$$

In the context of heterogeneity, however, the time-dependent optical linewidth is the important quantity [114, 115]. Because this Gaussian width is determined by inhomogeneous broadening, it characterizes the distribution of site specific energies which originates from the structural disorder of the supercooled liquid [78]. Accordingly, inhomogeneous optical linewidths and amplitudes of the Stokes shift are related via the fluctuation–dissipation theorem (FDT) in equilibrium systems [116] and solvation experiments access both the mean and variance of the relaxing quantity. In a dielectric measurement, the analogous information would be the entire distribution of molecular polarization states, instead of measuring the macroscopic average only.

It is easy to imagine that the linewidth would remain constant if each probe molecule experienced the same time-dependent red-shift, corresponding to homogeneous solvent dynamics. In the case of heterogeneous dynamics, probes at different sites will be subject to different solvent response times. At some intermediate time this results in some faster sites being near their equilibrium energy while other slow sites have remained near their initial energy, thereby giving rise to an increased linewidth relative to homogeneous dynamics. A simplified scheme of how heterogeneity generates this transient excess linewidth is shown in figure 7. The quantitative treatment of the linewidth in dynamically heterogeneous solvents has been supplied recently [117]. Designating $\sigma(t \to 0) = \sigma_0$ and $\sigma(t \to \infty) = \sigma_\infty$ and assuming that the local response can be written as a stretched exponential with 'intrinsic' exponent β_{intr}, a simple relation between $\sigma(t)$ and $C(t)$ can be established in the absence of rate exchange, with β_{intr} being the only unknown parameter:

$$\sigma^2_{het}(t) = \sigma^2_\infty + (\sigma^2_0 - \sigma^2_\infty)C(2^{1/\beta_{intr}}t) + \Delta^2\lfloor C(2^{1/\beta_{intr}}t) - C^2(t)\rfloor. \tag{9}$$

Note that this expression produces a peak in $\sigma_{het}(t)$, whereas homogeneous dynamics has always led to monotonic curves according to [118],

$$\sigma^2_{\rm hom}(t) = \sigma^2_\infty + (\sigma^2_0 - \sigma^2_\infty)C^2(t). \tag{10}$$

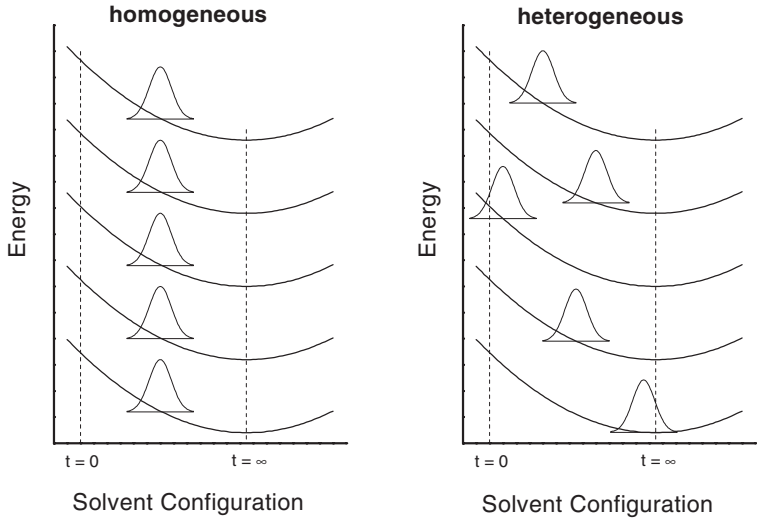

Figure 7. Schematic and simplified representation of spectral diffusion on the excited state potential surface at some intermediate time $0 < t_0 < \infty$ [122]. The curves are for five different sites with incremental energy offset for clarity. If subject to homogeneous dynamics, different sites will exhibit the same spectral shift at any time (left panel). In the heterogeneous case, the slow and fast sites display distinct spectral positions at t_0, which gives rise to a transient increase of the ensemble-averaged linewidth $\sigma(t)$ (right panel).

The effect of heterogeneous dynamics on time-resolved optical lines has been addressed explicitly by Matyushov [119]. For the particular case of $\sigma_\infty = \sigma_0$, the above relations reduce to $\sigma^2_{het}(t) = \sigma^2_\infty + \Delta^2\lfloor C(2^{1/\beta_{intr}}t) - C^2(t)\rfloor$ and $\sigma^2_{\rm hom}(t) = \sigma^2_\infty$; i.e., the signature of heterogeneity is a maximum in $\sigma(t)$ while homogeneity results in a time-invariant optical linewidth σ_∞. Figure 8 displays solvation results in terms of $C(t)$ and $\sigma(t)$ for the system quinoxaline (QX) in 2-methyl-tetrahydrofuran (MTHF) after mastering the curves obtained from different temperatures in the regime of time–temperature superposition. The time-resolved linewidth clearly indicates heterogeneity and a fit based on equation (9) reveals exponential local responses with $\beta_{intr} = 1.00 \pm 0.08$ [120]. Although this detailed analysis of optical lines has focused on the system QX/MTHF, peaks in $\sigma(t)$ have been observed in several other glass-forming materials.

That rate exchange can affect the relation between $\sigma(t)$ and $C(t)$ has been observed for a certain exchange model using simulation techniques in which relaxation and rate exchange are independent events [121, 122]. The independently chosen distributions for the α-relaxation times τ_α and rate exchange processes characterized by τ_x are tailored to obtain a satisfactory representation of the experimental $C(t)$ data and then $\sigma(t)$ is derived from the simulation using the same dynamic model. For this method of modelling dynamical disorder, an exchange parameter $Q = \langle\tau_x\rangle/\langle\tau_\alpha\rangle \leqslant 9$ combined with $\beta_{intr} = 1$ turns out to be incompatible with the observed linewidths. Diezemann has reported a dynamical model intrinsically associated with $Q = 1$ because it does not distinguish at all between relaxation and exchange events [123]. Although this model reproduces the observed linewidth data using $Q = 1$ and $\beta_{intr} = 1$, it is bound to remain incompatible with the values of $Q \gg 1$ observed directly for *ortho*-terphenyl via the deep photobleaching experiment performed by Ediger and co-workers [94–96] and discussed in section 3.2. In a further paper, Diezemann *et al* [124] have discussed a model of dynamics with a variable parameter γ_x for the 'exchange' rate, which reproduces the

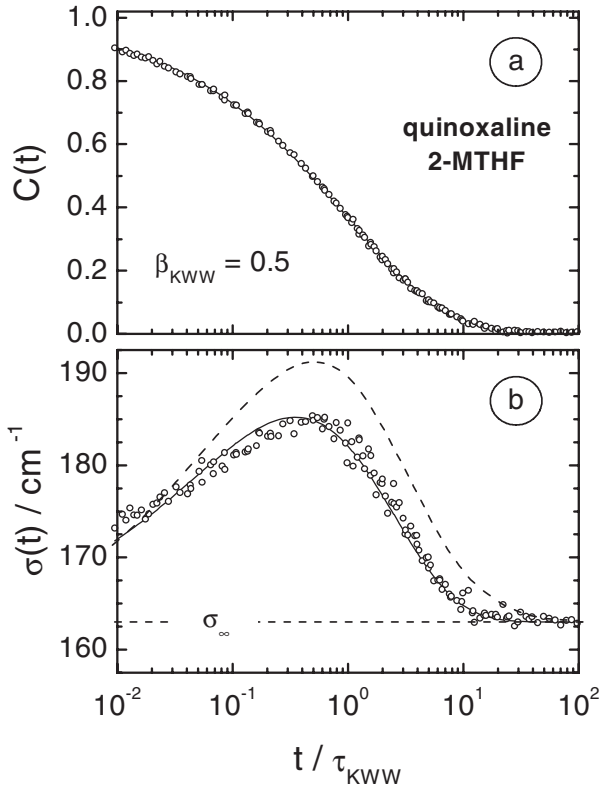

Figure 8. Master plot of the Stokes shift correlation function $C(t)$ (symbols, (a)) and of the inhomogeneous linewidth $\sigma(t)$ (symbols, (b)) versus t/τ_{KWW} for the solute QX in the solvent MTHF, measured at temperatures 91 K $\leqslant T \leqslant$ 97 K in steps of 1 K [120]. The solid curve in (a) is a fit to $C(t)$ using a stretched exponential, $C(t) = \exp[-(t/\tau_{KWW})^{0.5}]$. The solid curve in (b) is based upon a static distribution of intrinsically exponential relaxations, whereas homogeneity would lead to $\sigma(t) \equiv \sigma_\infty$. The dashed curve represents a simulation result for heterogeneous dynamics subject to rate exchange characterized by $Q = 2.8$ [121].

observed linewidth data $\sigma(t)$ for arbitrary γ_x. The feature that the time-resolved linewidths $\sigma(t)$ emerging from this model are γ_x invariant is solely a consequence of the Gaussian fluctuations implied in this approach. In these Langevin equations, the transition frequency of a 'slow' probe appears to depend on that of a 'fast' probe and vice versa, which is rather inapproapriate for the typical solvation experiment performed in the limit of non-interacting solute molecules.

The above lineshape measurement and analysis is also possible at significantly higher temperatures and faster dynamics. Coumarin 153, a fluorescent laser dye with excited state lifetime $\tau_{fl} \approx 6$ ns, is an appropriate probe for assessing heterogeneity in the nanosecond regime of MTHF [125]. In this case, the emission spectra are recorded in a time-integrated fashion and equations (9) and (10) are modified in order to account for the time-dependent emission intensity $I(t) \propto \exp(-t/\tau_{fl})$. As shown in figure 9, heterogeneity is again observed, although the structural relaxation time is a factor of 10^6 faster compared with the heterogeneous dynamics observed using the triplet probe QX in MTHF. Note that these short time experiments correspond to temperatures in excess of the MCT critical temperature $T_c \approx 107$ K for this liquid.

Again based on phosphorescence solvation dynamics experiments, Pastukhov *et al* [126] claim to have found evidence for large scale heterogeneity in terms of a clustered structure

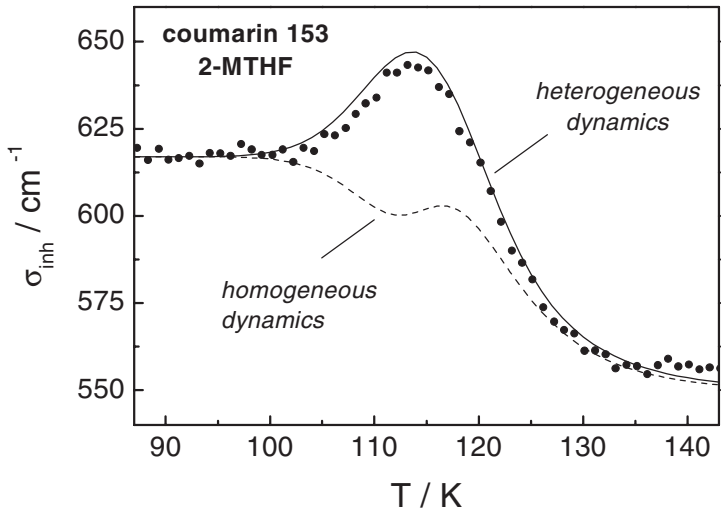

Figure 9. Inhomogeneous linewidth $\sigma_{inh}(T)$ of the fluorescence of Cu153 in MTHF as a function of temperature (symbols) [125]. The values are obtained by fitting the sum of four Gaussians to each spectrum, where the vibronic bands have a common linewidth σ_{inh} and energy separation $\nu_{vib} = 1300\ \mathrm{cm}^{-1}$. The curves represent $\sigma_{inh}(T)$ as expected for homogeneous (dashed) and for heterogeneous (solid) solvent dynamics. The calculations assume $\tau_{fl} = 6$ ns and $C(t) = \exp[-(t/\tau_{diel})^{\beta}]$ with $\beta = 0.8$ and $\tau_{diel}(T)$ taken from dielectric measurements [112].

with length scales of 1000 nm in a 94% glycerol–water mixture near its glass transition. Here, Rayleigh scattering from large scale density fluctuations is made responsible for the observed temperature dependence of the eosin emission intensities, while other sources of intensity variation are disregarded. Note that this system is not chemically homogeneous.

3.5. Translation–rotation decoupling

The coefficients of rotational and self-diffusion in the viscous regime of glass-formers are accessible via NMR measurements and field-gradient NMR techniques [127, 128]. Interestingly, these studies have shown that the temperature dependence of translational diffusion (D_{trans}) in the range $D_{trans} > 10^{-11}\ \mathrm{cm}^2\ \mathrm{s}^{-1}$ differs from that of rotational diffusion (D_{rot}) for temperatures $T < 1.2 \times T_g$, while $D_{trans}(T)$ and $D_{rot}(T)$ display the same behaviour at elevated temperatures, $T > 1.2 \times T_g$. In the lower temperature regime, $D_{trans}(T)$ displays a weaker temperature dependence relative to $D_{rot}(T)$ and, accordingly, translational diffusion is enhanced over rotation if compared with the higher temperature situation. Ediger and co-workers have confirmed these results in an extended temperature range by comparing rotational and translational motion of probe molecules in molecular [129] and polymeric [130] systems.

Within the framework of a dynamically homogeneous system, one would conclude on the counterintuitive picture of molecules moving an appreciable distance in real space yet without losing memory of their angular orientation [131]. However, the assumption of heterogeneity eliminates this problem [131–134]. Within this picture of spatially distributed timescales τ, one can argue that the average timescale of rotational motion is governed by the slower contributions within the (spatial) distribution of relaxation times, $D_{rot} \propto \langle\tau\rangle^{-1}$, while the faster times are more relevant in determining the average translation time with D_{trans} being approximated by $\langle\tau^{-1}\rangle$ [133]. As a consequence of this explanation, the extent of translational enhancement is expected to correlate with the width of the relaxation time distribution and should disappear as the net correlation function approaches a single exponential [135].

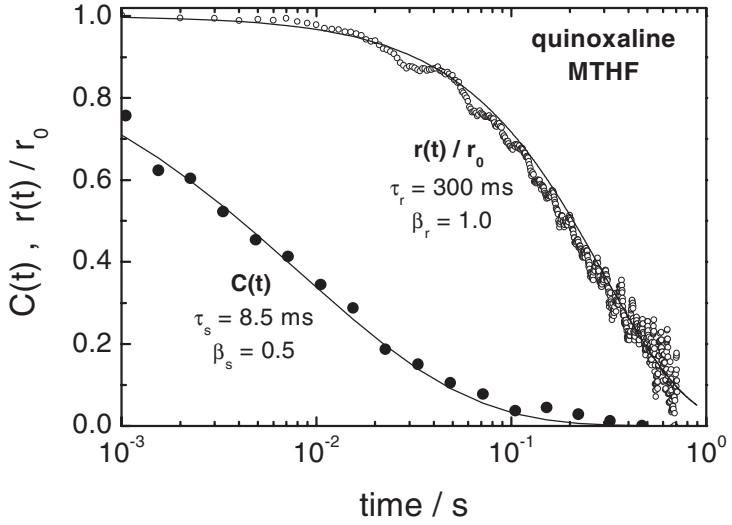

Figure 10. Solvation and probe rotation dynamics of quinoxaline in 2-methyl-tetrahydrofuran (MTHF) , measured simultaneously at $T = 92.0$ K [143]. Solid symbols refer to the magic angle Stokes shift correlation function $C(t)$, fitted by a stretched exponential with $\tau_s = 8.5$ ms and $\beta_s = 0.5$. Open symbols refer to the probe rotation correlation function $g_2(t) = r(t)/r_0$, fitted by a stretched exponential with $\tau_r = 300$ ms and $\beta_r = 1.0$.

3.6. Exponential probe rotation

The rotational correlation function of guest molecules in a glass-forming host environment has been studied by various techniques, for example fluorescence [136] and phosphorescence [137] depolarization, photobleaching [93], NMR [138–140] and dielectric relaxation [141]. Investigations of probe rotation as a function of the relative probe size reveal that the rotation of a guest which is larger than the host molecule is much slower and more exponential if compared with the dispersive host dynamics [142]. In terms of the stretched exponential parameters for guest and host dynamics, this means that $\beta_{guest} > \beta_{host}$ and $\tau_{guest} > \tau_{host}$, where $\beta_{guest} \approx 1$ is achieved already for guests which exceed the host size by a small amount. These features have been observed for relaxation times ranging from 10^{-10} to 10^4 s [142]. A recent study of optical depolarization combined with solvation dynamics experiments near T_g has demonstrated that these relations $\beta_{guest} > \beta_{host}$ and $\tau_{guest} > \tau_{host}$ apply also when comparing the rotation of larger guests with the dynamics of selectively those host molecules which are in the immediate vicinity of the guest site [143]. A representative comparison of an exponential probe rotation correlation function $r(t)/r_0$ with the Stokes shift correlation $C(t)$ originating from the dispersive solvent dynamics is shown in figure 10. For this simultaneous recording of $r(t)$ and $C(t)$, the solvation dynamics response $C(t)$ reflects the orientational motion of specifically those solvent dipoles (MTHF) which surround the larger probe (quinoxaline). Although the probe rotates slowly, its neighbouring solvent molecules retain their bulklike dynamics.

Two possibilities exist for explaining the exponential character of slowly rotating probes surrounded by faster and non-exponential dynamics:

(i) the larger probe size involves more distant host molecules in facilitating rotation (spatial average over the heterogeneous dynamics) and
(ii) the relaxation time around the probe fluctuates efficiently on the timescale of probe rotation (time average over heterogeneous dynamics via rate exchange).

Most results concerning rate exchange would be in accord with nearly exponential dynamics for a time average over an interval which exceeds the structural relaxation time by a factor of 20 or more, which is the situation observed experimentally. An exception is a study of rate exchange times in *ortho*-terphenyl very close to its glass transition [95], which would exclude time averaging as a source of probe rotation exponentiality [142]. In order to make spatial averaging responsible for $\beta_{guest} > \beta_{host}$, one needs to assume that the rotation of the probe involves the action of a sufficient number of host molecules such that probe reorientation averages over a spatial range within which the dynamics is representative for the entire ensemble. Without any assumptions about the details of heterogeneous dynamics, the present results are not decisive as regards the type of averaging responsible for exponential probe rotation. However, such probe rotation results imply constraints on the length scales and lifetimes associated with heterogeneous dynamics [128, 142, 143]. Clearly, either the spatial extent or the lifetime of a cluster with a specific relaxation time needs to be sufficiently small in order to account for exponential dynamics of a guest embedded in the highly dispersive dynamics of the host.

3.7. Microscopic observations

The examples of experimental approaches to heterogeneous dynamics discussed above all have in common that ensemble-averaged quantities are being measured. These experiments require the detection of large ensembles, which causes some difficulties in discriminating between homogeneous and heterogeneous scenarios. Observation of the dynamics on nanometre scales or even single-molecule detection offers insight into the microscopics of relaxation phenomena from a different perspective.

Israeloff and co-workers have used the tip of an atomic force microscope (AFM) for measuring the dielectric polarization noise of polyvinylacetate (PVAc) while probing a volume of only 2×10^{-17} cm^3 [144, 145]. The most striking observation is the occasional appearance of a Lorentzian contribution to the spectral density if the high frequency wing of the process is monitored over a few hours. Such a Lorentzian corresponds to a purely exponential relaxation, which appears to fluctuate on the timescale of the average structural relaxation time, i.e. its lifetime is long compared with its relaxation time constant. This experiment demonstrates heterogeneity and the existence of rate exchange in a very direct manner. Additionally, random telegraph switching was observed, where the polarization appears to favour a small number of preferred levels. The authors conclude that the polarization fluctuation originates from larger angle orientational jumps of some effective dipole, whose strength is that of several PVAc monomer dipoles [145]. The results suggest that the observed polarization is dominated by a single cluster or CRR, perhaps the size of a few nanometres, if the detection is confined to a sufficiently small volume and to a frequency range in which the density of relaxing units is low.

Analogous to molecular liquids, colloidal systems can assume liquid, glassy and crystalline phases. In these materials, the density instead of temperature is the most relevant variable for controlling the thermodynamic state. Below a certain density, particles become trapped within the cage determined by their neighbours, which constitutes the colloidal glass transition. Typical colloidal particles exhibit radii of 1 μm with little polydispersity. If dyed with appropriate labels, their motion can be monitored in real space as a function of time by rapid imaging through a confocal microscope. The resulting movies are then analysed to yield time-resolved mean squared displacements and, more importantly, velocity and direction correlations of particle pairs or clusters.

Rice and co-workers [146] have studied particle trajectories in colloidal liquids. In these quasi-two-dimensional systems, it has been found that transient ordered domains are

separated by more disordered boundaries which display faster stringlike particle motion. These dynamical heterogeneities are seen to correlate with structural fluctuations. A three-dimensional colloidal glass-former has been investigated by Weeks and co-workers [147]. In the supercooled fluid near its colloidal glass transition, fast particles are spatially clustered and neighbouring particle pairs preferentially move along the same direction. The size of these clusters grows as the density is increased towards the value at which the colloidal glass transition occurs. Although these features are reminiscent of the Adam–Gibbs theory [25], the relation between cooperatively rearranging regions and dynamical clusters remains to be clarified. Additionally, these clusters are subject to rate exchange which restores ergodicity at longer times.

Single-molecule spectroscopy has made significant advances since its first demonstration by Moerner [148]. There are several ways to extract information about local dynamics from this technique. First, subtle dynamics which remains active even in low temperature glasses is reflected in spectral diffusion, often associated with tunnelling states [75, 76]. Second, the fluorescence lifetime of dye molecules can be very sensitive to the local viscosity around the probe through motionally activated channels of radiationless transitions. Based on this effect, Ishikawa *et al* [149] have proposed triphenylmethane as a probe for studying heterogeneities as regards the local viscosity in liquids and polymers. Finally, Deschenes and Vanden Bout [150] have adopted the technique [151] of measuring the rotational dynamics of isolated dye molecules in a glass-forming host. Assuming that the reduced linear dichroism of a single molecule may be analysed like an isotropic ensemble, these authors conclude that isolated rhodamine 6G dye molecules in a polymethylacrylate (PMA) matrix perform diffusive rotational motion which is altered by environmental exchange on a longer timescale. The extent to which these probes are coupled to the matrix dynamics is unclear, so that the observed heterogeneity is not necessarily a reflection of the behaviour of the PMA matrix.

3.8. Molecular dynamics simulations

Computer simulations of molecular dynamics (MD) aimed at investigating dynamic heterogeneity have been carried out for a variety of different model systems, for example hard and soft spheres, binary Lennard-Jones mixtures and models of polymer melts [72]. Computer time typically limits the accessible range of such calculations to $T > T_c$, i.e. to near or above the critical temperature of the mode-coupling theory. The analysis of such simulations focuses on measuring how far particles are displaced during a given time interval and observing correlated dynamics of particle pairs or within clusters, equivalent to evaluating higher order correlation functions [152]. It is observed that fast and slow particles are spatially clustered, indicative of heterogeneity in models of simple liquids [153–156] and polymer melts [157, 158].

An example of such clusters seen in the MD simulation of an equilibrium binary Lennard-Jones liquids is displayed in figure 11. The picture shows only the slowest 5% and fastest 5% of the majority particles, which obviously form spatial clusters. In these model systems, this transient structure regarding the dynamics exhibits no clear correlation with density fluctuations. Interestingly, the length scales of dynamical correlation increase as the temperature is lowered [159,160]. Within the clusters of correlated timescales, strings of highly cooperative motion are observed in which a particle tends to replace its moving neighbour. Additionally, these model liquids display a decoupling of diffusion from the structural relaxation time, assumed to originate from the heterogeneous nature of the dynamics. This feature is much like the rotation–translation decoupling measured in real liquids, but noticeable in the MD results already at temperatures which exceed the onset of decoupling derived from experiment. Because Lennard-Jones mixtures and polydisperse colloidal fluids are comparable

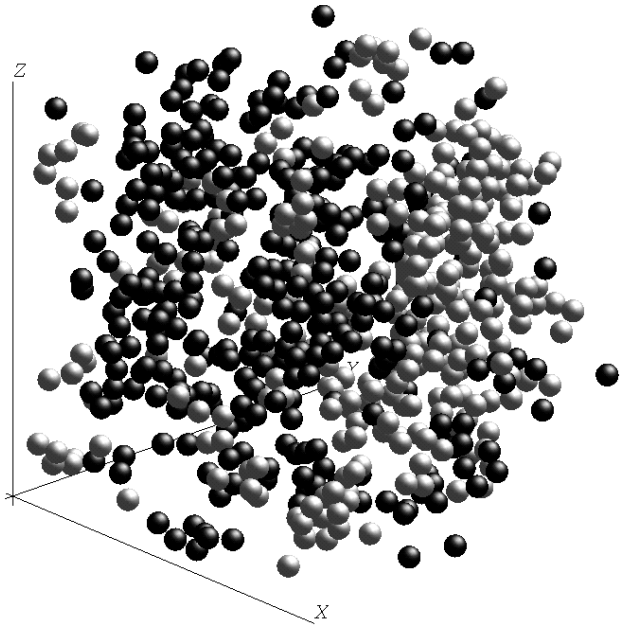

Figure 11. Snapshot of a simulated glass-forming 80:20 binary Lennard-Jones mixture containing 8000 particles. The temperature of this equilibrium system is just above the ideal mode-coupling temperature T_c. Only the 5% most mobile (light grey) and 5% least mobile (dark grey) majority particles in a given time interval are shown. Evidently, these dynamical subsets form spatial clusters. Reprinted with permission from [160].

systems, there is a strong similarity of the respective observations [72]. Whether the heterogeneities seen in MD simulations develop gradually into those observed experimentally in molecular and polymeric melts near T_g is still unclear. Although heterogeneous dynamics of a molecular liquid has been observed in the time and temperature regime accessible to MD simulations, no details such as length scales or exchange times are currently available from experiments in the nanosecond or $T > T_c$ range for a more detailed comparison [125].

3.9. Models of hetergeneous dynamics

Models in which some thermodynamic variable fluctuates in space were proposed long before dynamic heterogeneity was observed by experiment. Provided that the random variable controls the local relaxation time, such approaches can be considered models of heterogeneous dynamics. In a number of theories, characteristic length scales ξ_H of distinguishable subsystems within the liquid are being associated with the pronounced increase in apparent activation energy as the temperature is decreased. Examples are Bueche's treatment of thermal fluctuations [161–163], the liquid-like clusters of Cohen and Grest [164], the cooperatively rearranging regions of the Adam–Gibbs theory [25] and the thermodynamic fluctuations approach by Donth [165, 166]. The latter also establishes a link between the length scale ξ_C of cooperative motion and the width of the probability density of relaxation times, such that ξ_C is accessible to experiment via the relaxation pattern. These models suggest that much of the deviation between the temperature dependence of the structural relaxation time and simple activated behaviour originates from an increasing length scale ξ_C as T_g is approached.

More recent models of heterogeneous dynamics have addressed additional aspects of the supercooled liquid phenomenology. The model of 'dynamically correlated domains' advanced by Chamberlin assumes a distribution of domain sizes with the relaxation time increasing exponentially with inverse size and with a relaxation strength that is proportional to the size [167]. The approach is based upon mean-field theory applied to finite clusters yielding an activation energy similar to the Curie–Weiss law. The model does not imply any divergence of the relaxation time at temperatures $T > 0$ because finite size effects suppress a sharp transition [168]. Averaging over the domain size distribution leads to VFT type behaviour together with frequency-dependent susceptibilities which are in accord with non-exponential relaxation data, including the typical deviation from power law behaviour at high frequencies [169]. Different approaches partition the liquid into two distinct subsets, like the 'two-fluid' model of Bendler and Shlesinger [170]. A similar molecular picture has led Fischer to a model of 'heterophase fluctuations', assuming the coexistence of liquid-like and amorphous solid-like clusters in the liquid [171]. Thermodynamic considerations of this two-phase system establish the temperature dependence of the fraction of the liquid-like phase, which is an important factor in predicting the variation of average relaxation times with temperature. Appropriate adjustment of the parameters of this model replicates experimental temperature dependences of the structural relaxation time over a wide range of dynamics. Again using a very different approach, Kivelson and Tarjus [172] have devised a model of 'frustration-limited domains'. Here, short range interactions which tend to induce extended domains of a preferred structure as in spin systems compete with weaker long range interactions, which frustrate the size of ordered domains and thereby avoid the critical point. The resulting distribution of domain sizes and size specific relaxation times gives rise to non-exponential and super-Arrhenius relaxation behaviour, in agreement with the dielectric responses of real materials. Heterogeneous orientational dynamics of the primary relaxation has also been discussed in the framework of activated processes in a free-energy landscape, where it is concluded that no separate timescale for exchange is required for rationalizing higher order time correlation functions as measured by multi-dimensional NMR techniques [173]. Recently, Long has proposed a model of heterogeneous dynamics, in which the glass transition is associated with the percolation of slow domains [174]. The dynamic scaling approach of Colby is capable of reproducing the dramatic slowing down of the dynamics with decreasing temperature [42]. This theory has recently been extended to evaluating temperature-dependent length scales of cooperativity [175]. Finally, it will be noted that the distribution of 'initial states' discussed by Halpern is not considered a real source of heterogeneity [176].

A recurring pattern in these models of dynamics in supercooled liquids is the increasing number of sites that become trapped in the slowly relaxing domains as the temperature is lowered towards the glass transition. Thereby, the heterogeneous nature of the structural relaxation is being related to one of the most prominent features of viscous melts, i.e. with the substantial temperature dependence of the apparent activation energy in fragile glass-formers. Less encouraging is the number of models which all explain non-exponential and non-Arrhenius dynamics on the basis of fundamentally different ways of invoking heterogeneity.

4. Discussion

Although the idea of spatial fluctuations regarding relaxation dynamics in viscous melts is older, it has been mainly the last 10 years in which experimental results on single-component materials have been accumulated which are incompatible with homogeneity regarding structural relaxations [54,68–70]. Below we compile the results of such experiments, sorted according to their statement concerning the various aspects of heterogeneity.

4.1. Heterogeneity in liquids

Most of the approaches to heterogeneous dynamics are targeted at the primary or α-relaxations of molecular and polymeric melts, which involve larger scale rearrangements of the molecular structure and eventually give rise to viscous flow. As detailed above, the most important techniques in this field are multi-dimensional NMR, deep photobleaching, dielectric hole burning (DHB), solvation dynamics (SD), translation–rotation decoupling (TRD), exponential probe rotation (PR) and microscopic observations. Evidence for heterogeneous structural relaxations in molecular liquids has been established for *ortho*-terphenyl by NMR [15, 85, 86], PB [93–95], TRD [128, 129] and PR [142], for glycerol by NMR [89, 177] and DHB [97, 98], for propylene carbonate by NMR [178] and DHB [102], for toluene by NMR [179] and for 2-methyl-tetrahydrofuran by SD [114, 120], PR [143] and NMR [180]. Polymer systems investigated include polyvinylacetate by NMR [14, 82, 87] and AFM-probed polarization noise [144, 145], polystyrene by NMR [83, 87, 88], PB [96], TRD [130, 131], PR [96] and anomalous diffusion [199] and polymethylacrylate by single-molecule spectroscopy [150]. The investigations compiled above all refer to the viscous regime with relaxation times $\tau > 1$ ms, equivalent to temperatures not far away from T_g. Indications of heterogeneous dynamics in the regime of nanoseconds are thus far restricted to the observation of exponential rotation of large probes in *ortho*-terphenyl [142], the solvation dynamics study of 2-methyl-tetrahydrofuran in the nanosecond regime [125] and the simulation results on model liquids and polymers [72]. According to these results, heterogeneity has been observed across a broad range of materials, varying significantly in their glass transition temperature, fragility, polarity and chemical composition. Other dynamical processes identified as heterogeneous are those in colloidal liquids [146, 147], magnetic spin glasses [106] and relaxor ferroelectrics [105].

Generally accepted evidence for a dynamically homogeneous α-relaxation has not been reported thus far. Two claims for homogeneous dynamics can be found in the literature. One is an solvation dynamics study which exploited the fact the predictions of molecular theories of solvation do depend on the nature of the dynamics, homogeneous versus heterogeneous [13, 181]. Subsequently, it has been recognized that the difference in these predictions is small compared with the uncertainties arising from the simplifications inherent in the mean spherical approximation [182] theory of dipolar solvation. A second such case is the neutron scattering study reported by Arbe *et al* [183], which concludes on homogeneity on the basis of the observed q-dependence of the relaxation time τ_{KWW} in polymeric materials. On the other hand, Heuer and Spiess have argued that the findings are not decisive regarding the nature of the dynamics [184].

Towards higher temperature and faster dynamics, supercooled molecular liquids tend to display practically exponential relaxation patterns. Obviously, an exponentially relaxing liquid is intrinsically homogeneous because spectral selectivity cannot be performed with only a single relaxation time. Because all experiments performed on non-exponential primary relaxations have concluded on heterogeneity, one might ask whether the measurements would detect homogeneous behaviour if present. It has been only for dielectric hole burning on a vitreous ionic conductor [104], where both heterogeneous and homogeneous dynamics could be identified (see section 4.2) in terms of the respective presence and lack of spectral selectivity. Therefore, it seem justified to assume that all non-exponential relaxations are associated with heterogeneous dynamics.

4.2. Heterogeneity in glasses

In the glassy state below T_g, larger scale molecular rearrangements similar to those of the α-relaxation are frozen, if physical aging is disregarded. The most prominent dynamical

feature in vitreous materials is the Johari–Goldstein (JG) or slow β-relaxation, usually related to localized librational motion within the otherwise rigid cage of surrounding molecules [48,49]. It is easily imagined that the spatial structure responsible for heterogeneous dynamics above T_g becomes frozen in the glassy state and gives rise to heterogeneity of the secondary JG type relaxation. NMR experiments have concluded on the heterogeneous nature of the JG process based on the non-exponential character of spin–lattice relaxation [185, 186]. Spectral selectivity within the broad distribution of JG type relaxation times has been demonstrated by dielectric hole burning experiments on vitreous D-sorbitol [103]. This heterogeneity of the secondary process in a D-sorbitol glass is long lived compared with the relaxation time of the modified subensemble, but a more quantitative assessment of rate exchange below T_g is not available. Practically static heterogeneity is anticipated at temperatures sufficiently below T_g if primary structural relaxation is required in order to promote rate exchange.

Heterogeneity has also been observed regarding the dynamics of isomerization [187,188] and racemization [189] kinetics of probe molecules in glassy polymer matrices. Although there is no obvious relation to the heterogeneous dynamics of primary relaxations, these sub-T_g observations demonstrate that structural and compositional disorder greatly affects the dynamics of processes embedded in these glassy matrices. The occurrence of motional heterogeneities as well as rate exchange regarding small molecules in a binary liquid close to its glass transition has been demonstrated by solid state two-dimensional NMR [138].

A different kind of dynamics in glassy materials is that of ion diffusivity, which gives rise to time- or frequency-dependent conductivity $\sigma^*(\omega)$. If viewed in a modulus representation, $M''(\omega)$ versus $\log(\omega)$, the signature of dispersive ion motion is reminiscent of the broadened and asymmetrical loss peaks $\varepsilon''(\omega)$ originating from dielectric relaxation [190,191]. Dielectric hole burning using modulus detection has been performed on $2Ca(NO_3)_2 \cdot 3KNO_3$ (CKN) at $T = T_g - 33$ K, i.e. in the structurally frozen state [104]. In this experiment, heterogeneous diffusivity has been observed at high frequencies, whereas a crossover towards homogeneous dynamics occurred at lower frequencies. The lack of spectral selectivity at longer timescales is assumed to originate from the spatial averaging, promoted by the increase of the mean square displacement as the frequency is lowered to the point where the conductivity changes from ac to dc character. It is this ionic conductor CKN for which Moynihan had predicted heterogeneous ion dynamics on the basis of light scattering experiments which are suggestive of heterogeneous dynamics [192].

4.3. Intrinsic non-exponentiality

A number of investigations can be found which are aimed at measuring the degree of heterogeneity [15, 193]. Such a scale attempts to discriminate the contributions to the non-exponentiality of the average correlation decay $\phi(t)$. The two contributions are easily quantified if a KWW type overall relaxation with stretching parameter β_{KWW} is modelled by a superposition of intrinsically non-exponential decays with KWW exponent $\beta_{intr} \geqslant \beta_{KWW}$,

$$\phi(t) = \exp[-(t/\tau_{KWW})^{\beta_{KWW}}] = \int_0^\infty g(\tau) \exp[-(t/\tau)^{\beta_{intr}}]\, \mathrm{d}\tau = \langle \exp[-(t/\tau)^{\beta_{intr}}] \rangle. \qquad (11)$$

Intrinsically exponential contributions with $\beta_{intr} = 1$ lead to the heterogeneous limit in which the dispersion of $\phi(t)$ originates solely from the probability density $g(\tau)$ or spatial distribution of relaxation times τ. In the homogeneous extreme, the overall dispersion is inherent in each relaxing unit, $\beta_{intr} = \beta_{KWW}$, thereby eliminating the spatial distribution of relaxation times, i.e. $g(\tau) = \delta(\tau - \tau_{KWW})$. One possibility for establishing a normalized continuous scale for

intermediate situations is given by [15]

$$\eta = \frac{\beta_{intr} - \beta_{KWW}}{1 - \beta_{KWW}}. \tag{12}$$

Similar measures for the degree of heterogeneity associated with relaxation functions other than the KWW type can easily be established in an analogous fashion.

Regarding materials of low molecular weight, studies reporting on the value of β_{intr} include propylene carbonate investigated by dielectric hole burning at $T = T_g + 4$ K ($\tau = 100$ ms, $\beta_{KWW} = 0.72$) [102] and *ortho*-terphenyl using multi-dimensional NMR techniques at $T = T_g + 11$ K ($\tau = 16$ ms, $\beta_{KWW} = 0.42$) [15]. In these two cases, the experimental observations are compatible with the purely heterogeneous case, $\beta_{intr} = 1$. Solvation dynamics studies on MTHF in the range $T = T_g \ldots T_g + 6$ K ($\tau = 27$ s $\ldots$ 1.5 ms, $\beta_{KWW} = 0.50$) reveal exponential local responses with $\beta_{intr} = 1.00 \pm 0.08$ [120] across this experimental range.

Multi-dimensional NMR techniques have also determined the degree of heterogeneity for polymeric systems, polystyrene (PS) at $T = T_g + 13$ K ($\tau = 6.5$ ms, $\beta_{KWW} = 0.45$) and polyvinylacetate (PVAc) at $T = T_g + 10$ K ($\tau = 20$ ms, $\beta_{KWW} = 0.52$) [87]. The conclusion for these polymers is that their intrinsic segmental relaxation is associated with back-jump probabilities $R \approx 0.3 \pm 0.1$ for PS and $R \approx 0.4 \pm 0.05$ for PVAc. Values of $R > 0$ are introduced in order to model intrinsically non-exponential relaxation regarding the angular correlation function of polymer segments. Based on the empirical relation $\beta_{intr} \approx 1 - R/2$ valid within the range $0 \leqslant R \leqslant 0.6$, the above values of R translate into $\beta_{intr} \approx 0.85$ ($\eta = 0.73$) for PS and $\beta_{intr} \approx 0.80$($\eta = 0.58$) for PVAc. Based on these results, it appears that glass-forming materials of low molecular weight are associated with pure heterogeneity, $\beta_{intr} = 1$ or $\eta = 1$, while polymeric systems exhibit homogeneous contributions with respect to their segmental reorientation.

4.4. Spatial aspects

The observation of heterogeneity, for example via spectral selectivity, implies the coexistence of (to some extent independent) relaxation times which contribute in a parallel rather than serial fashion. Without further evidence for spatial structuring on a characteristic length scale ξ_H, spectral selectivity itself does not necessarily involve a spatial variation of timescales. Identifying heterogeneity with spatially fluctuating dynamics is often based on intuition and on the difficulties in imagining heterogeneous dynamics without a spatial distribution in real molecular systems. Recently, Cugliandolo and Iguain [194, 195] have claimed that a non-spatial system is capable of reproducing the features observed in dielectric hole burning experiments. Although non-zero difference signals $\Delta\phi(t)$ could be obtained, this infinite range interaction model did not succeed in demonstrating spectral selectivity and heterogeneity [196]. Additionally, the relevance of this model has been questioned on the basis of its out-of-equilibrium type dynamics [197]. Furthermore, the spatial character of heterogeneity has never been claimed on the basis of dielectric hole burning results.

It is important to discriminate the experimental results according to their ability to identify the *spatial* character of heterogeneity unambiguously. The first experiment to quantify a length scale of heterogeneity ξ_H is that of Tracht *et al* [88], which combined the multi-dimensional NMR with the effect of spin diffusion. The conclusion of that work is that the slow dynamics of polyvinylacetate at $T = T_g + 10$ K is clustered and that the cluster diameter is $\xi_H = 3$ nm. Additional data and a revised analysis have led to $\xi_H = 3 \pm 1$ nm for both polyvinylacetate and *ortho*-terphenyl [198]. A similar measurement has been performed subsequently on the molecular glass-former glycerol by Reinsberg *et al* [89], resulting in a

scale of $\xi_H \approx 1$ nm. Solvation dynamics results suggest a lower limit to the length scale within which the relaxation times are practically identical. The correlation function $C(t)$ observed in this experiment reflects the orientational dynamics averaged over the first solvent shell, i.e. over the ≈10 nearest neighbours. Recall that individual solvation probe molecules experience exponential dynamics with $\beta_{intr} = 1.00 \pm 0.08$ [120]. From the exponentiality of this subensemble it has been concluded that all molecules within the first solvent shell contribute with the same timescale [113]. The exponential rotation correlation functions of larger probe molecules also give a hint towards the spatial scale involved in heterogeneous dynamics, but only in combination with the timescale of rate exchange. Whether time or space averaging is responsible for this exponentiality remains to be clarified. Therefore, it is only in the case of sufficiently slow rate exchange that one can correlate the effective size of an exponentially rotating probe with the scale required to achieve sufficient spatial averaging [127,142,143]. The size of heterogeneous domains has also been inferred from the observation of anomalous tracer diffusion in PS, indicative of a transition from Fickian to non-Fickian diffusion. Modelling this dynamics on heterogeneous lattices has led Wang and Ediger [199] to the conclusion that these heterogeneities are associated with length scales around 2 nm.

Information regarding the spatial aspect of heterogeneity also comes from the microscopic observations on colloidal liquids [146,147] and from MD simulation results [159,160]. In both cases, the length scales grow as the temperature is lowered towards the critical temperature T_c. For molecular liquids and polymers, however, no experimental results are available concerning how the characteristic length scales of heterogeneous dynamics change with temperature in the range $T_g \ldots T_c$. It has also remained uncertain how the length scale ξ_H of heterogeneity relates to the length ξ_C involved in the concept of cooperativity, although the numbers reported for both lengths are around a few nanometres.

Experimentally, no spatial fluctuation of a separate quantity has been identified which can be made responsible for the spatial variations of timescales. Obvious candidates for such sources of heterogeneous dynamics are fluctuations in density or locally preferred molecular structures which could modulate the dynamics. Because the dynamics of molecules is extremely sensitive to those variables, their fluctuation amplitudes are possibly too small to be detected by available techniques. MD simulations have also been employed to seek for correlations between dynamics and other local variables. In model liquids, the only correlation established is that between local relaxation time and potential energy [200].

4.5. Rate exchange effects

The aspect of persistence time is perhaps the most controversial issue in the context of heterogeneous dynamics. A number of terms have been used to address the timescales involved in heterogeneity. If heterogeneity is regarded as disorder with respect to relaxation time, then 'dynamical disorder' is appropriate to express that a slow site eventually becomes a fast one and vice versa [201]. The 'exchange time' τ_x refers to the time it takes a particular site to change its relaxation timescale due to the effect of some usually unspecified environmental variable. Accordingly, 'memory time' is the time a site memorizes its initial timescale. A further term intended to express the same feature is 'heterogeneity lifetime', which is not supposed to imply that the dynamics becomes more homogeneous at longer times. It is reasonable and customary to compare results for the exchange time τ_x on a scale relative to the relaxation time τ_α of the α-process. Because in general both τ_x and τ_α are distributed rather than single-valued quantities, the memory parameter Q is best expressed by the ratio of their average values [83],

$$Q = \frac{\langle \tau_x \rangle}{\langle \tau_\alpha \rangle}. \tag{13}$$

It is important to discriminate the cases where $\langle\tau_\alpha\rangle$ refers to the distribution of the total ensemble from those where $\langle\tau_\alpha\rangle$ refers to the spectrally selected subensemble and the respective designations $\langle\tau_\alpha\rangle_{tot}$ and $\langle\tau_\alpha\rangle_{sel}$ are introduced here. In the original definition of the rate memory parameter Q given by Heuer, a two-state model has been considered where always the slow processes are selected, i.e. $Q = \langle\tau_x\rangle/\langle\tau_\alpha\rangle_{slow}$ [83]. In this manner, Q states the average number of slow relaxation events before an exchange process occurs.

If $\langle\tau_x\rangle$ is identical to $\langle\tau_\alpha\rangle_{tot}$, then the exchange mechanism does not add a new timescale to the dynamics of liquids. In the case of so-called long lived heterogeneity, $\langle\tau_x\rangle > \langle\tau_\alpha\rangle_{tot}$, heterogeneity introduces a further timescale which exceeds that of the α-process [95]. In any case, the time $\langle\tau_x\rangle$ sets a lower limit for the structural relaxation time in the strict sense, because 'dynamical structure' arising from site specific time constants persists until the exchange mechanism has established ergodicity. We should also be aware of the fact that the value of $\langle\tau_x\rangle$ and even the distribution of τ_x do not specify much of the actual exchange process. Because very little is known about the molecular mechanisms involved in rate exchange, numerous possibilities of how to model exchange are being considered. The changes of a time constant τ_α at a certain site can be thought of as a diffusion or random walk process along the relaxation time axis. The site could perform a jump in τ_α space to a nearby value with a high probability to revert to the initial state. In this case, a large number of such displacements is necessary in order for that site to fully lose correlation with the $t = 0$ situation. Alternatively, subsequent values of τ_α could be modelled by picking random numbers from the τ_α-distribution, implying that the time constant correlation is lost entirely with every jump. Modelling relaxation and exchange as independent events has been proposed in terms of coupled Fokker–Planck equations beginning with a two-site picture in which only fast and slow sites are considered [202, 203]. A typical trajectory of a relaxing quantity subject to such an exchange process is depicted in figure 12, showing that modelling relaxation and exchange as distinct events preserves the continuous character of the trajectories. In real systems, it is not necessarily the case that rate exchange events occur totally independent of the correlation decay of the α-process. For instance, the time τ_x a site memorizes its current τ_α could be a function of τ_α itself or relaxation processes can be assumed to trigger rate exchange and vice versa.

Independent of the particular model, rate exchange leads to a difference between the underlying 'true' or 'static' distribution of relaxation times τ_α and the effective or observable distribution. The latter is based upon fitting the correlation decay by a superposition of exponentials according to equation (2). A rate constant τ_α which is slower than exchange will never be observed because those sites will preferentially relax via exchange to a faster value of τ_α. Accordingly, the probability density of relaxation times, $g(\tau)$, in equation (2) is determined by both the 'true' distribution of τ_α and the exchange effects unless $\langle\tau_x\rangle \gg \langle\tau_\alpha\rangle$. Allowing for intrinsic non-exponentiality, $\beta_{intr} < 1$, in the presence of rate exchange complicates the situation further.

The first experimental assessment of exchange times has been reported by Spiess and co-workers [14, 82] for polyvinylacetate at a temperature $T = T_g + 20$ K using a reduced 4D-NMR method, which resulted in $Q = 1$ [204]. For polystyrene at $T = T_g + 10$ K, Kuebler *et al* [83] arrived at $Q = 1$ on the basis of solid state NMR echo techniques. Cicerone and Ediger [94] found $Q \approx 100$ for supercooled *ortho*-terphenyl (OTP) at $T = T_g + 1$ K using the dynamically selective photobleaching method. For the same material but at a higher temperature, $T = T_g + 10$ K, Böhmer *et al* [85] reported $Q \approx 1$ based on multi-dimensional NMR measurements. More recently, Wang and Ediger [95] have shown that Q decays gradually from 540 to 2 in OTP as the temperature increases from T_g to $T_g + 10$ K. This strong decrease of Q with increasing temperature eliminates the apparent discrepancy between $Q > 100$ and $Q \approx 1$ obtained for the same material. Dynamical heterogeneities

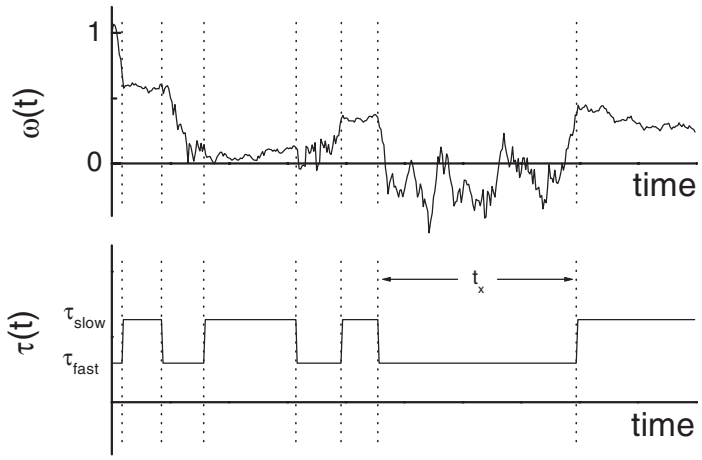

Figure 12. A typical trajectory of a fluctuating observable $\omega(t)$ subject to rate exchange [121]. The calculation is based on two relaxation times $\tau_{fast} = 0.3$ and $\tau_{slow} = 10$ with rate exchange time $\tau_x = 2$ and equal probability for a site to reside in either state. The lower panel indicates the fluctuating time constant for this trajectory, with the dashed vertical lines marking the actual times of rate exchange. In this particular model the trajectories remain continuous because relaxation and exchange events are assumed to be independent processes.

observed in dielectric hole burning experiments on propylene carbonate and glycerol by Schiener *et al* [97, 98] have been associated with $Q \approx 1$. According to these observations, dynamical heterogeneities in supercooled molecular liquids appear to be longer lived only in the immediate vicinity of the glass transition temperature. The result $Q > 9$ derived from analysing solvation dynamics data of 2-methyl-tetrahydrofuran (MTHF) in the range $T_g \leqslant T \leqslant T_g + 6$ K within the framework of a particular exchange model does not seem to follow the trend of $Q(T)$ mentioned above [121, 122]. A very recent NMR study of the rotational correlation function of MTHF arrived at $Q \approx 1$ on the ms timescale [180], i.e. within the range for which $Q > 9$ was found for the Stokes-shift correlation function of quinoxaline (QX) as the solute in MTHF. If the correlation functions of these two different experiments were comparable, the logical conclusion would be to disqualify the exchange model employed for concluding on $Q > 9$. On the other hand, the NMR experiment observes the single-particle rotational correlation in neat MTHF, while the solvation dynamics technique reveals the collective orientational response of the solvent in the immediate vicinity of the QX probe. From the probe rotation studies discussed in section 3.6 and shown in figure 10 we learned that QX rotates a factor of 35 slower compared with the solvent response in the case of MTHF. If rate exchange requires a substantial mobility of all molecules within the spatial range of the heterogeneity length scale, then one may speculate that a slowly rotating probe frustrates nearby rate exchange. In this case, the Q resulting from solvation studies is a matter of the solute/solvent size relation [143]. Although this issue is not resolved, the MTHF studies are likely to enhance our understanding of exchange mechanisms. At present, the experimental results do not lead to a simple picture concerning rate exchange.

Persistence times of rate constants have also been reported for the microscopically probed polarization of polyvinylacetate using atomic force microscopy [145]. In contrast to most other cases of spectral selectivity, this experiment focused on the contributions at high frequencies relative to the average relaxation time. Time constants were observed to fluctuate on the average

timescale of the α-relaxation, $\langle\tau_x\rangle \approx \langle\tau_\alpha\rangle_{tot}$, and therefore slowly relative to their individual relaxation time, $\langle\tau_x\rangle \gg \langle\tau_\alpha\rangle_{sel}$. At least for the high frequency wing of the distribution, this result contrasts the picture that rate exchange is always triggered by a relaxation event.

A note of caution applies to comparing the above Q values, especially those derived from different experimental methods. The majority of results associated with multi-dimensional NMR compare the exchange time with the average relaxation time of the selected slow subensemble, where as a function of filter efficiency the ratio $\langle\tau_\alpha\rangle_{sel}/\langle\tau_\alpha\rangle$ typically varies from 2 to 10. In other spectrally selective experiments, the subensemble can refer to the faster than average particles. For the deep photobleaching experiments of Ediger and co-workers, the selected subensemble is only 30% slower than the full ensemble, so that discriminating between $\langle\tau_\alpha\rangle_{sel}$ and $\langle\tau_\alpha\rangle$ is of little relevance. In the case of the solvation dynamics experiments, no spectral selection is being performed, i.e. the 'selected' and full ensembles are identical in this case. As a consequence, the rate memory parameter Q is not being used consistently throughout the literature.

5. Concluding remarks

Within the past ten years, overwhelming evidence for heterogeneity regarding non-exponential relaxation in single-component systems has been accumulated from a variety of experimental techniques. Heterogeneous dynamics has been observed in both the primary (α-) and secondary (slow β-) relaxation processes. The studies include materials such as molecular liquids, polymeric melts, a relaxor ferroelectric and a vitreous ionic conductor, all differing considerably in their fragility, glass transition temperature, relaxation time dispersion, polarity and chemical constitution. Experiments have identified the heterogeneous nature of relaxation processes which range in timescale from $\approx 10^2$ s ($T \approx T_g$) to $\approx 10^{-9}$ s ($T > T_c$). Based on these observations, non-exponential relaxations appear to be heterogeneous without exception. Few of these experiments are capable of assigning a length scale to heterogeneous dynamics, reporting spatial dimensions of several nanometres. Therefore, non-exponentiality translates not only into the coexistence of different timescales, but into the understanding that relaxation time is a spatially varying quantity. Accordingly, characterizing a liquid by a certain viscosity captures only a fraction of the complex behaviour in real liquids. This structure regarding the timescales of molecular motion is transient, i.e. the time constants fluctuate in both space and time, as required by ergodicity in the equilibrium state. Although rate exchange *per se* is being observed, the nature and timescale of this rate exchange mechanism remains to be clarified.

Obviously, it is tempting to correlate the spatial fluctuation of the dynamics with those of other quantities, like density or locally preferred structures. Attempts to identify such correlations experimentally have thus far been unsuccessful, but simulation work has related timescales to local potential energies. Typical non-exponential correlation functions exhibit time constants which cover several orders of magnitude. Apart from polymeric melts, this distribution of timescales is understood as originating from a superposition of intrinsically exponential contributions. Therefore, the spatial fluctuation of whatever quantity is responsible for the heterogeneity has to account for the entire relaxation time dispersion, usually covering many decades in time or frequency.

The motivation for studying dynamical processes on microscopic rather than macroscopic scales has led to a number of novel experimental techniques, MD simulations and models of relaxation phenomena. Regarding our insight into the microscopic features of relaxation phenomena, significant progress has been made in recent years. Still, many unresolved questions and controversies remain to be addressed in future work.

Acknowledgments

I am grateful for the contributions of my collaborators in the field of heterogeneous dynamics, in particular H Wagner, H Wendt and M Yang. It is a pleasure to thank C A Angell, H Bässler, R Böhmer, R V Chamberlin, M D Ediger, E W Fischer, J T Fourkas, A Heuer, J Klafter, M Maroncelli, B Nickel, H Sillescu and J L Skinner for valuable discussions.

References

[1] Angell C A, Ngai K L, McKenna G B, McMillan P F and Martin S W 2000 Relaxation in glassforming liquids and amorphous solids *J. Appl. Phys.* **88** 3113
[2] Elliott S R 1983 *Physics of Amorphous Materials* (London: Longman)
[3] Jäckle J 1986 Models of the glass transition *Rep. Prog. Phys.* **49** 171
[4] Richert R and Blumen A (eds) 1994 *Disorder Effects on Relaxational Processes* (Berlin: Springer)
[5] Ngai K L and Wright G B (eds) 1991 Relaxations in complex systems *J. Non-Cryst. Solids* **131–133**
[6] Ngai K L, Riande E and Wright G B (eds) 1994 Relaxations in complex systems *J. Non-Cryst. Solids* **172–174**
[7] Ngai K L, Riande E and Ingram M D (eds) 1998 Relaxations in complex systems *J. Non-Cryst. Solids* **235–237**
[8] Angell C A, Ngai K L, Kieffer J, Egami T and Nienhaus G U (eds) 1997 Structure and dynamics of glasses and glass formers *Mater. Res. Soc. Symp. Proc.* **455**
[9] Fourkas J T, Kivelson D, Mohanty U and Nelson K A (eds) 1997 *Supercooled Liquids: Advances and Novel Applications* (Washington, DC: American Chemical Society)
[10] Williams G 1978 Time-correlation functions and molecular motion *Chem. Soc. Rev.* **7** 89
[11] Kohlrausch R 1854 Theorie des elektrischen Rückstandes in der Leidener Flasche *Prog. Ann. Phys.* **91** 179
[12] Williams G and Watts D C 1970 Non-symmetrical dielectric relaxation behaviour arising from a simple empirical decay function *Trans. Faraday Soc.* **66** 80
[13] Richert R 1993 Origin of dispersion in dipolar relaxations of glasses *Chem. Phys. Lett.* **216** 223
[14] Schmidt-Rohr K and Spiess H W 1991 Nature of nonexponential loss of correlation above the glass transition investigated by multi-dimensional NMR *Phys. Rev. Lett.* **66** 3020
[15] Böhmer R *et al* 1998 Nature of the non-exponential primary relaxation in structural glass-formers probed by dynamically selective experiments *J. Non-Cryst. Solids* **235–237** 1
[16] Vogel H 1921 Das Temperaturabhängigkeitsgesetz der Viskosität von Flüssigkeiten *Phys. Z.* **22** 645
[17] Fulcher G S 1923 Analysis of recent measurements of the viscosity of glasses *J. Am. Ceram. Soc.* **8** 339
[18] Tammann G and Hesse W 1926 Die Abhängigkeit der Viskosität von der Temperatur bei unterkühlten Flüssigkeiten *Z. Anorg. Allg. Chem.* **156** 245
[19] Williams M L, Landel R F and Ferry J D 1953 The temperature dependence of relaxation mechanisms in amorphous polymers and other glass-forming liquids *J. Am. Ceram. Soc.* **77** 3701
[20] Angell C A 1991 Relaxation in liquids, polymers and plastic crystals—strong/fragile patterns and problems *J. Non-Cryst. Solids* **131–133** 15
[21] Stein D L and Palmer R G 1988 Nature of the glass transition *Phys. Rev.* B **38** 12 035
[22] Cohen M H and Turnbull D 1959 Molecular transport in liquids and glasses *J. Chem. Phys.* **31** 1164
[23] Cohen M H and Grest G S 1979 Liquid–glass transition, a free-volume approach *Phys. Rev.* B **20** 1077
[24] Goldstein M 1973 Viscous liquids and the glass transition. IV. Thermodynamic equations and the transition *J. Phys. Chem.* **77** 667
[25] Adam G and Gibbs J H 1965 On the temperature dependence of cooperative relaxation properties in glass-forming liquids *J. Chem. Phys.* **43** 139
[26] Takahara S, Yamamuro O and Suga H 1994 Heat capacities and glass transitions of 1-propanol and 3-methylpentane under pressure. New evidence for the entropy theory *J. Non-Cryst. Solids* **171** 259
[27] Chang S S and Bestul A B 1972 Heat capacity and thermodynamic properties of *o*-terphenyl crystal, glass, and liquid *J. Chem. Phys.* **56** 503
[28] Sethna J P 1988 Speculations on the glass transition *Europhys. Lett.* **6** 529
[29] Fischer E W, Donth E and Steffen W 1992 Temperature dependence of characteristic length for glass transition *Phys. Rev. Lett.* **68** 2344
[30] Rizos A K and Ngai K L 1997 Cooperative length scale of Aroclor near its dynamic glass transition *Mater. Res. Soc. Symp. Proc.* **455** 141
[31] Richert R 1996 Geometrical confinement and cooperativity in supercooled liquids studied by solvation dynamics *Phys. Rev.* B **54** 15 762

[32] Hempel E, Hempel G, Hensel A, Schick C and Donth E 2000 Characteristic length of dynamic glass transition near T_g for a wide assortment of glass-forming substances *J. Phys. Chem.* B **104** 2460
[33] Souletie J 1994 Hierarchical scaling: an analytical approach to slow relaxations in spin glasses, glasses, and other correlated systems *J. Appl. Phys.* **75** 5512
[34] Souletie J 1994 An analytical approach of the ergodic–non-ergodic transition in correlated systems *J. Non-Cryst. Solids* **172–174** 108
[35] Yamamuro O, Tsukushi I, Lindqvist A, Takahara S, Ishikawa M and Matsuo T 1998 Calorimetric study of glassy and liquid toluene and ethylbenzene: thermodynamic approach to spatial heterogeneity in glass-forming molecular liquids *J. Phys. Chem.* B **102** 1605
[36] Bendler J T and Shlesinger M F 1988 Generalized Vogel law for glass-forming liquids *J. Stat. Phys.* **53** 531
[37] Ferry J D, Grandine L D and Fitzgerald E R 1953 The relaxation distribution function of polyisobutylene in the transition from rubber-like to glass-like behaviour *J. Appl. Phys.* **24** 911
[38] Bässler H 1987 Viscous flow in supercooled liquids analyzed in terms of transport theory for random media with energetic disorder *Phys. Rev. Lett.* **58** 767
[39] Richert R and Bässler H 1990 Dynamics of supercooled melts treated in terms of the random walk concept *J. Phys.: Condens. Matter* **2** 2273
[40] Souletie J 1990 The glass transition: dynamic and static scaling approach *J. Physique* I **51** 883
[41] Souletie J and Bertrand D 1991 Glasses and spin glasses: a parallel *J. Physique* **1** 1627
[42] Colby R H 2000 Dynamic scaling approach to glass formation *Phys. Rev.* E **61** 1783
[43] Götze W and Sjögren L 1992 Relaxation processes in supercooled liquids *Rep. Prog. Phys.* **55** 241
[44] Barlow A J, Lamb J and Matheson 1966 Viscous behaviour of supercooled liquids *Proc. R. Soc.* A **292** 322
[45] Stickel F, Fischer E W and Richert R 1995 Dynamics of glass-forming liquids: I. Temperature-derivative analysis of dielectric relaxation data *J. Chem. Phys.* **102** 6251
[46] Stickel F, Fischer E W and Richert R 1996 Dynamics of glass-forming liquids: II. Detailed comparison of dielectric relaxation, DC-conductivity and viscosity data *J. Chem. Phys.* **104** 2043
[47] Richert R and Angell C A 1998 Dynamics of glass-forming liquids. V. On the link between molecular dynamics and configurational entropy *J. Chem. Phys.* **108** 9016
[48] Johari G P and Goldstein M 1970 Viscous liquids and the glass transition: II. Secondary relaxations in glasses of rigid molecules *J. Chem. Phys.* **53** 2372
[49] Johari G P and Goldstein M 1971 Viscous liquids and the glass transition: III. Secondary relaxations in aliphatic alcohols and other nonrigid molecules *J. Chem. Phys.* **55** 4245
[50] Hansen C, Stickel F, Berger T, Richert R and Fischer E W 1997 Dynamics of glass-forming liquids. III. Comparing the dielectric α- and β-relaxation of 1-propanol and *o*-terphenyl *J. Chem. Phys.* **107** 1086
[51] Goldstein M 1969 Viscous liquids and the glass transition: a potential energy barrier picture *J. Chem. Phys.* **51** 3728
[52] Schönhals A 2001 Evidence for a universal crossover behaviour of the dynamic glass transition *Europhys. Lett.* **56** 815
[53] Hansen C, Stickel F, Richert R and Fischer E W 1998 Dynamics of glass-forming liquids. IV. True activated behaviour above 2 GHz in the dielectric α-relaxation of organic liquids *J. Chem. Phys.* **108** 6408
[54] Ediger M D, Angell C A and Nagel S R 1996 Supercooled liquids and glasses *J. Phys. Chem.* **100** 13 200
[55] Palmer G, Stein D, Abrahams E and Anderson P W 1984 Models of hierarchically constrained dynamics for glassy relaxation *Phys. Rev. Lett.* **53** 958
[56] Ngai K L 1979 Universality of low-frequency fluctuation, dissipation and relaxation properties of condensed matter. I *Comments Solid State Phys.* **9** 127
[57] Ngai K L 1979 Universality of low-frequency fluctuation, dissipation and relaxation properties of condensed matter. II *Comments Solid State Phys.* **9** 141
[58] Ngai K L and White C T 1979 Frequency dependence of dielectric loss in condensed matter *Phys. Rev.* B **20** 2475
[59] Havriliak S and Negami S 1966 A complex plane analysis of α-dispersions in some polymer systems *J. Polym. Sci.: Polym. Symp.* **14** 99
[60] Glöckle W G and Nonnenmacher T F 1991 Fractional integral operators and Fox functions in the theory of viscoelasticity *Macromol.* **24** 6426
[61] Metzler R and Klafter J 2000 The random walk's guide to anomalous diffusion: a fractional dynamics approach *Phys. Rep.* **339** 1
[62] Hilfer R (ed) 2000 *Applications of Fractional Calculus in Physics* (Singapore: World Scientific)
[63] Hilfer R 2002 Experimental evidence for fractional time evolution in glass forming materials *Chem. Phys.* at press
[64] Matsuoka S 1992 *Relaxation Phenomena in Polymers* (Munich: Hanser)

[65] Olsen N B, Dyre J C and Christensen T 2001 Time–temperature superposition in viscous liquids *Phys. Rev. Lett.* **86** 1271
[66] Böhmer R, Ngai K L, Angell C A and Plazek D J 1993 Nonexponential relaxations in strong and fragile glass formers *J. Chem. Phys.* **99** 4201
[67] Böhmer R and Angell C A 1994 Local and global relaxations in glass-forming materials *Disorder Effects on Relaxational Processes* ed R Richert and A Blumen (Berlin: Springer)
[68] Ediger M D 2000 Spatially heterogeneous dynamics in supercooled liquids *Annu. Rev. Phys. Chem.* **51** 99
[69] Sillescu H 1999 Heterogeneity at the glass transition: a review *J. Non-Cryst. Solids* **243** 81
[70] Böhmer R 1998 Non-exponential relaxation in disordered materials: phenomenological correlations and spectrally selective experiments *Phase Transitions* **65** 211
[71] Böhmer R 1998 Nanoscale heterogeneity of glass-forming liquids: experimental advances *Curr. Opin. Solid State Mater. Sci.* **3** 378
[72] Glotzer S C 2000 Spatially heterogeneous dynamics in liquids: insights from simulation *J. Non-Cryst. Solids* **274** 342
[73] Böhmer R, Schiener B, Hemberger J and Chamberlin R V 1995 Pulsed dielectric spectroscopy of supercooled liquids *Z. Phys.* B **99** 91
[74] Böhmer R, Schiener B and Hemberger J 1996 Pulsed dielectric spectroscopy of supercooled liquids *Z. Phys.* B **99** 624 (erratum)
[75] Moerner W E (ed) 1987 *Persistent Spectral Hole Burning: Science and Applications* (Berlin: Springer)
[76] Jankowiak R and Small G J 1987 Hole-burning spectroscopy and relaxation dynamics of amorphous solids at low temperatures *Science* **237** 618
[77] Machida S, Tanaka S, Horie K and Li B 1999 Low-temperature relaxation of polymers around doped dyes studied by persistent spectral hole burning *J. Polym. Sci.* B **37** 585
[78] Galley W C and Purkey R M 1970 Role of heterogeneity of the solvation site in electronic spectra in solution *Proc. Natl Acad. Sci. USA* **67** 1116
[79] Ormos P, Ansari A, Braunstein D, Cowen B R, Frauenfelder H, Hong M K, Iben I E T, Sauke T B, Steinbach P J and Young R D 1990 Inhomogeneous broadening in spectral bands of carbonmonoxymyoglobin. The connection between spectral and functional heterogeneity *Biophys. J.* **57** 191
[80] Diezemann G and Schirmacher W 1990 High-field nuclear spin relaxation in liquids and solids *J. Physique* **2** 6681
[81] Schnauss W, Fujara F, Hartmann K and Sillescu H 1990 Nonexponential ^{2}H spin–lattice relaxation as a signature of the glassy state *Chem. Phys. Lett.* **166** 381
[82] Heuer A, Wilhelm M, Zimmermann H and Spiess H W 1995 Rate memory of structural relaxation in glasses and its detection by multi-dimensional NMR *Phys. Rev. Lett.* **75** 2851
[83] Kuebler S C, Heuer A and Spiess H W 1997 Glass transition of polymers: memory effects in structural relaxation of PS *Phys. Rev.* E **56** 741
[84] Heuer A 1997 Information content of multitime correlation functions for the interpretation of structural relaxation in glass-forming systems *Phys. Rev.* E **56** 730
[85] Böhmer R, Hinze G, Diezemann G, Geil B and Sillescu H 1996 Dynamic heterogeneity in supercooled *ortho*-terphenyl studied by multi-dimensional deuteron NMR *Europhys. Lett.* **36** 55
[86] Böhmer R, Diezemann G, Hinze G and Sillescu H 1998 A nuclear magnetic resonance study of higher-order correlation functions in supercooled *ortho*-terphenyl *J. Chem. Phys.* **108** 890
[87] Heuer A, Tracht U, Kuebler S C and Spiess H W 1999 The orientational memory from three-time correlations in multi-dimensional NMR experiments *J. Mol. Struct.* **479** 251
[88] Tracht U, Wilhelm M, Heuer A, Feng H, Schmidt-Rohr K and Spiess H W 1998 Length scale of dynamic heterogeneities at the glass transition determined by multi-dimensional nuclear magnetic resonance *Phys. Rev. Lett.* **81** 2727
[89] Reinsberg S A, Qiu X H, Wilhelm M, Spiess H W and Ediger M D 2001 Length scale of dynamics heterogeneity in supercooled glycerol near T_g *J. Chem. Phys.* **114** 7299
[90] Schmidt-Rohr K and Spiess H W 1994 *Multi-Dimensional Solid-State NMR and Polymers* (London: Academic)
[91] Spiess H W and Schmidt-Rohr K 1994 Molecular dynamics in polymers from multi-dimensional NMR *Disorder Effects on Relaxational Processes* ed R Richert and A Blumen (Berlin: Springer)
[92] Böhmer R, Diezemann G, Hinze G and Rössler E 2001 Dynamics of supercooled liquids and glassy solids *Prog. NMR Spectrosc.* **39** 191
[93] Cicerone M T and Ediger M D 1993 Photobleaching technique for measuring ultraslow reorientation near and below the glass transition: tetracene in *o*-terphenyl *J. Chem. Phys.* **97** 10 489
[94] Cicerone M T and Ediger M D 1995 Relaxation of spatially heterogeneous dynamic domains in supercooled *ortho*-terphenyl *J. Chem. Phys.* **103** 5684

[95] Wang C-Y and Ediger M D 1999 How long do regions of different dynamics persist in supercooled *ortho*-terphenyl *J. Phys. Chem.* B **103** 4177
[96] Wang C-Y and Ediger M D 2000 Lifetime of spatially heterogeneous dynamic domains in polystyrene melts *J. Chem. Phys.* **112** 6933
[97] Schiener B, Böhmer R, Loidl A and Chamberlin R V 1996 Nonresonant spectral hole burning in the slow dielectric response of supercooled liquids *Science* **274** 752
[98] Schiener B, Chamberlin R V, Diezemann G and Böhmer R 1997 Nonresonant dielectric hole burning spectroscopy of supercooled liquids *J. Phys. Chem.* **107** 7746
[99] Diezemann G 2001 Response theory for nonresonant hole burning: stochastic dynamics *Europhys. Lett.* **53** 604
[100] Böhmer R and Diezemann G 2002 Principles and applications of pulsed dielectric spectroscopy and nonresonant dielectric hole burning *Broadband Dielectric Spectroscopy* ed F Kremer and A Schönhals (Berlin: Springer)
[101] Richert R 2002 The modulus of dielectric and conductive materials and its modification by high electric fields *J. Non-Cryst. Solids*, at press
[102] Chamberlin R V, Schiener B and Böhmer R 1997 Slow dielectric relaxation of supercooled liquids investigated by nonresonant spectral hole burning *Mater. Res. Soc. Symp. Proc.* **455** 117
[103] Richert R 2001 Spectral selectivity in the slow β-relaxation of a molecular glass *Europhys. Lett.* **54** 767
[104] Richert R and Böhmer R 1999 Heterogeneous and homogeneous diffusivity in an ion-conducting glass *Phys. Rev. Lett.* **83** 4337
[105] Kircher O, Schiener B and Böhmer R 1998 Long-lived dynamic heterogeneity in a relaxor ferroelectric *Phys. Rev. Lett.* **81** 4520
[106] Chamberlin R V 1999 Nonresonant spectral hole burning in a spin glass *Phys. Rev. Lett.* **83** 5134
[107] McKenna G B and Zapas L J 1985 The superposition of small deformations on large deformations: measurements of the incremental relaxation modulus for a polyisobutylene solution *J. Polym. Sci.: Polym. Phys. Ed.* **23** 1647
[108] McKenna G B and Zapas L J 1986 Superposition of small strains on large deformations as a probe of nonlinear response in polymers *Polym. Eng. Sci.* **26** 725
[109] Ware W R, Lee S K, Brant G J and Chow P 1971 Nanosecond time-resolved emission spectroscopy: spectral shifts due to solvent-excited solute relaxation *J. Chem. Phys.* **54** 4729
[110] Maroncelli M 1993 The dynamics of solvation in polar liquids *J. Mol. Liq.* **57** 1
[111] Maroncelli M and Fleming G R 1987 Picosecond solvation dynamics of coumarin 153: the importance of molecular aspects of solvation *J. Chem. Phys.* **86** 6221
[112] Richert R, Stickel F, Fee R S and Maroncelli M 1994 Solvation dynamics and the dielectric response in a glass-forming solvent: from picoseconds to seconds *Chem. Phys. Lett.* **229** 302
[113] Richert R 2000 Triplet state solvation dynamics: basics and applications *J. Chem. Phys.* **113** 8404
[114] Richert R 1997 Evidence for dynamic heterogeneity near T_g from the time resolved inhomogeneous broadening of optical line shapes *J. Phys. Chem.* B **101** 6323
[115] Richert R and Richert M 1998 Dynamic heterogeneity, spatially distributed stretched-exponential patterns, and transient dispersions in solvation dynamics *Phys. Rev.* E **58** 779
[116] Loring R F 1990 Statistical mechanical calculation of inhomogeneously broadened absorption line shapes in solution *J. Phys. Chem.* **94** 513
[117] Richert R 2001 Theory of time dependent optical linewidths in supercooled liquids *J. Chem. Phys.* **114** 7471
[118] Stevens M D, Saven J G and Skinner J L 1997 Molecular theory of electronic spectroscopy in nonpolar fluids: ultrafast solvation dynamics and absorption and emission line shapes *J. Chem. Phys.* **106** 2129
[119] Matyushov D V 2001 Time-resolved fluorescence of polarizable chromophores *J. Chem. Phys.* **115** 8933
[120] Wendt H and Richert R 2000 Heterogeneous relaxation patterns in supercooled liquids studied by solvation dynamics *Phys. Rev.* E **61** 1722
[121] Richert R 2001 Spectral diffusion in liquids with fluctuating solvent responses: dynamical heterogeneity and rate exchange *J. Chem. Phys.* **115** 1429
[122] Richert R 2002 Heterogeneous solvent dynamics and time-resolved optical linewidths *J. Non-Cryst. Solids*, at press
[123] Diezemann G 2002 Time-dependent optical linewidth in fluctuating environments: stochastic models *J. Chem. Phys.* **116** 1647
[124] Diezemann G, Hinze G and Sillescu H 2002 Stochastic models for heterogeneous relaxation: application to inhomogeneous optical lineshapes *J. Non-Cryst. Solids*, at press
[125] Yang M and Richert R 2001 Observation of heterogeneity in the nanosecond dynamics of a liquid *J. Chem. Phys.* **115** 2676

[126] Pastukhov A V, Khudyakov D V, Vogel V R and Kotelnikov A I 2001 A supercooled glycerol–water mixture: evidence for the large-scale heterogeneity? *Chem. Phys. Lett.* **346** 61
[127] Fujara F, Geil B, Sillescu H and Fleischer G 1992 Translational and rotational diffusion in supercooled orthoterphenyl close to the glass transition *Z. Phys.* B **88** 195
[128] Chang I and Sillescu H 1997 Heterogeneity at the glass transition: translational and rotational self-diffusion *J. Phys. Chem.* B **101** 8794
[129] Cicerone M T and Ediger M D 1996 Enhanced translation of probe molecules in supercooled *o*-terphenyl: signature of spatially heterogeneous dynamics? *J. Chem. Phys.* **104** 7210
[130] Wang C-Y and Ediger M D 1997 Enhanced translational diffusion of 9,10-bis(phenylethynyl)anthracene (BPEA) in polystyrene *Macromol.* **30** 4770
[131] Cicerone M T, Blackburn F R and Ediger M D 1995 Anomalous diffusion of probe molecules in polystyrene: evidence for spatially heterogeneous segmental dynamics *Macromol.* **28** 8224
[132] Tarjus G and Kivelson D 1995 Breakdown of the Stokes–Einstein relation in supercooled liquids *J. Chem. Phys.* **103** 3071
[133] Cicerone M T, Wagner P A and Ediger M D 1997 Translational diffusion on heterogeneous lattices: a model for dynamics in glass forming liquids *J. Phys. Chem.* B **101** 8727
[134] Ediger M D 1998 Can density or entropy fluctuations explain enhanced translational diffusion in glass-forming liquids? *J. Non-Cryst. Solids* **235–237** 10
[135] Hall D B, Dhinojwala A and Torkelson J M 1997 Translation–rotation paradox for diffusion in glass-forming polymers: the role of the temperature dependence of the relaxation time distribution *Phys. Rev. Lett.* **79** 103
[136] Horng M-L, Gardecki J A and Maroncelli M 1997 Rotational dynamics of coumarin 153: time-dependent friction, dielectric friction, and other nonhydrodynamic effects *J. Phys. Chem.* A **101** 1030
[137] Nickel B and Ruth A A 1991 Phosphorescence from phenazine in alkane solvents in the glass transition range: spin–lattice, environment, and orientation relaxation of molecules in the metastable triplet state *J. Phys. Chem.* **95** 2027
[138] Vogel M and Rössler E 1998 Exchange processes in disordered systems studied by solid-state 2D NMR *J. Phys. Chem.* A **102** 2102
[139] Rössler E, Taupitz M and Vieth H M 1990 Heterogeneous spin–lattice relaxation revealing the activation energy distribution of mobile guests in organic glasses *J. Phys. Chem.* **94** 6879
[140] Roggatz I, Rössler E, Taupitz M and Richert R 1996 Non-exponential ^{2}H spin–lattice relaxation and slow translational exchange in disordered systems *J. Phys. Chem.* **100** 12 193
[141] Williams G and Hains P J 1971 Molecular motion in the supercooled liquid state: small molecules in slow motion *Chem. Phys. Lett.* **10** 585
[142] Cicerone M T, Blackburn F R and Ediger M D 1995 How do molecules move near Tg? Molecular rotation of six probes in *O*-terphenyl across 14 decades in time *J. Chem. Phys.* **102** 471
[143] Yang M and Richert R 2002 Solvation dynamics and probe rotation in glass-forming liquids *Chem. Phys.*, at press
[144] Vidal Russell E, Israeloff N E, Walther L E and Alvarez Gomariz H 1998 Nanometer scale dielectric fluctuations at the glass transition *Phys. Rev. Lett.* **81** 1461
[145] Vidal Russell E and Israeloff N E 2000 Direct observation of molecular cooperativity near the glass transition *Nature* **408** 695
[146] Cui B, Lin B and Rice S A 2001 Dynamical heterogeneity in a dense quasi-two-dimensional colloidal liquid *J. Chem. Phys.* **114** 9142
[147] Weeks E R, Crocker J C, Levitt A C, Schofield A and Weitz D A 2000 Three-dimensional direct imaging of structural relaxation near the colloidal glass transition *Science* **287** 627
[148] Moerner W E 1994 Examining nanoenvironments in solids on the scale of a single, isolated impurity molecule *Science* **265** 46
[149] Ishikawa M, Ye J Y, Maruyama Y and Nakatsuka H 1999 Triphenylmethane dyes revealing heterogeneity of their nanoenvironment: femtosecond, picosecond, and single-molecule studies *J. Phys. Chem.* A **103** 4319
[150] Deschenes L A and Vanden Bout D A 2001 Single-molecule studies of heterogeneous dynamics in polymer melts near the glass transition *Science* **292** 255
[151] Fourkas J T 2001 Rapid determination of the three-dimensional orientation of single molecules *Opt. Lett.* **26** 211
[152] Glotzer S C, Novikov V N and Schrøder T B 2000 Time-dependent, four-point density correlation function description of dynamical heterogeneity and decoupling in supercooled liquids *J. Chem. Phys.* **112** 509
[153] Kob W, Donati C, Plimpton S J, Poole P H and Glotzer S C 1997 Dynamical heterogeneities in a supercooled Lennard-Jones liquid *Phys. Rev. Lett.* **79** 2827

[154] Donati C, Douglas J F, Kob W, Plimpton S J, Poole P H and Glotzer S C 1998 Stringlike cooperative motion in a supercooled liquid *Phys. Rev. Lett.* **80** 2338
[155] Yamamoto R and Onuki A 1997 Kinetic heterogeneity in a highly supercooled liquid *J. Phys. Soc. Japan* **66** 2545
[156] Yamamoto R and Onuki A 1998 Heterogeneous diffusion in highly supercooled liquids *Phys. Rev. Lett.* **81** 4915
[157] Kanaya T, Tsukushi I, Kaji K, Gabrys B and Bennington S M 1998 Heterogeneity of amorphous polymers with various fragility indices as studied in terms of non-Gaussian parameter *J. Non-Cryst. Solids* **235–237** 212
[158] Kanaya T, Tsukushi I and Kaji K 1997 Non-Gaussian parameter and heterogeneity of amorphous polymers *Prog. Theor. Phys. Suppl.* **126** 133
[159] Bennemann C, Donati C, Baschnagel J and Glotzer S C 1999 Growing range of correlated motion in a polymer melt on cooling towards the glass transition *Nature* **399** 246
[160] Glotzer S C and Donati C 1999 Quantifying spatially heterogeneous dynamics in computer simulations of glass-forming liquids *J. Phys.: Condens. Matter* **11** A 285
[161] Bueche F 1953 Segmental mobility of polymers near their glass temperature *J. Chem. Phys.* **21** 1850
[162] Bueche F 1956 Derivation of the WLF equation for the mobility of molecules in molten glasses *J. Chem. Phys.* **24** 418
[163] Bueche F 1959 Mobility of molecules in liquids near the glass temperature *J. Chem. Phys.* **30** 748
[164] Grest G S and Cohen M H 1981 Liquids, glasses, and the glass transition: a free-volume approach *Adv. Chem. Phys.* **48** 455
[165] Donth E 1992 *Relaxation and Thermodynamics in Polymers* (Berlin: Akademie)
[166] Donth E 1996 Exhausting of fluctuating free volume of dynamic glass transition at low temperatures *J. Physique* **6** 1189
[167] Chamberlin R V 1993 Non-Arrhenius response of glass-forming liquids *Phys. Rev.* B **48** 15 638
[168] Chamberlin R V 1999 Mesoscopic mean-field theory for supercooled liquids and the glass transition *Phys. Rev. Lett.* **82** 2520
[169] Hansen C, Richert R and Fischer E W 1997 Dielectric loss spectra of organic glass formers and Chamberlin cluster model *J. Non-Cryst. Solids* **215** 293
[170] Bendler J T and Shlesinger M F 1992 Defect diffusion and a two-fluid model for structural relaxation near the glass–liquid transition *J. Phys. Chem.* **96** 3970
[171] Fischer E W, Bakai A S, Patkowski A, Steffen W and Reinhardt L 2002 Heterophase fluctuations in supercooled liquids and polymers *J. Non-Cryst. Solids*, at press
[172] Viot P, Tarjus G and Kivelson D 2000 A heterogeneous picture of α relaxation for fragile supercooled liquids *J. Chem. Phys.* **112** 10 368
[173] Diezemann G 1997 A free-energy landscape model for primary relaxation in glass-forming liquids: rotations and dynamic heterogeneities *J. Chem. Phys.* **107** 10 112
[174] Long D and Lequeux F 2001 Heterogeneous dynamics at the glass transition in van der Waals liquids, in the bulk and in thin films *Eur. Phys. J.* E **4** 371
[175] Erwin B M and Colby R 2002 Temperature dependences of viscosity and the length scale of cooperative motion for glass-forming liquids *J. Non-Cryst. Solids*, at press
[176] Halpern V 2002 Inhomogeneities as a result of non-exponential relaxation in disordered systems *J. Phys.: Condens. Matter* **14** 2475
[177] Hinze G, Diezemann G and Sillescu H 1998 Four-time rotational correlation functions *Europhys. Lett.* **44** 565
[178] Qi F, Schug K U, Dupont S, Döß A, Böhmer R, Sillescu H, Kolshorn H and Zimmermann H 2000 Structural relaxation of the fragile glass-former propylene carbonate studied by nuclear magnetic resonance *J. Chem. Phys.* **112** 9455
[179] Hinze G 1998 Geometry and timescale of the rotational dynamics in supercooled toluene *Phys. Rev.* E **57** 2010
[180] Qi F, El Goresy T, Döß A, Blochowicz T, Diezemann G, Hinze G, Zimmermann H, Sillescu H and Böhmer R 2002 Long-lived dynamic heterogeneities near the glass transition of simple supercooled liquids? *Europhys. Lett.* submitted
[181] Richert R 1994 Homogeneous dispersion of dielectric responses in a simple glass *J. Non-Cryst. Solids* **172–174** 209
[182] Rips I, Klafter J and Jortner J 1988 Solvation dynamics in polar liquids *J. Chem. Phys.* **89** 4288
[183] Arbe A, Colmenero J, Monkenbusch M and Richter D 1998 Dynamics of glass-forming polymers: 'homogeneous' versus 'heterogeneous' scenario *Phys. Rev. Lett.* **81** 590
[184] Heuer A and Spiess H W 1999 Comment on 'Dynamics of glass-forming polymers: 'homogeneous' versus 'heterogeneous' scenario' *Phys. Rev. Lett.* **82** 1335

[185] Schnauss W, Fujara F and Sillescu H 1992 The molecular dynamics around the glass transition and in the glassy state of molecular organic systems: a ^{2}H–nuclear magnetic resonance study *J. Chem. Phys.* **97** 1378
[186] Böhmer R, Hinze G, Jörg T, Qi F and Sillescu H 2000 Dynamical heterogeneity in α- and β-relaxations of glass forming liquids as seen by deuteron NMR *J. Phys.: Condens. Matter* **12** 383
[187] Richert R 1988 Merocyanine—spiropyran photochemical transformation in polymers, probing effects of random matrices *Macromol.* **21** 923
[188] Richert R and Heuer A 1997 Rate-memory and dynamic heterogeneity of first-order reactions in a polymer matrix *Macromol.* **30** 4038
[189] Park J-W, Ediger M D and Green M M 2001 Chiral studies in amorphous solids: the effect of the polymeric glassy state on the racemization kinetics of bridged paddled binaphthyls *J. Am. Chem. Soc.* **123** 49
[190] Macedo P B, Moynihan C T and Bose R 1972 The role of ionic diffusion in polarisation in vitreous ionic conductors *Phys. Chem. Glasses* **13** 171
[191] Wagner H and Richert R 1999 Measurement and analysis of time-domain electric field relaxation: the vitreous ionic conductor 0.4 $Ca(NO_3)_2$–0.6 KNO_3 *J. Appl. Phys.* **85** 1750
[192] Moynihan C T 1998 Description and analysis of electrical relaxation data for ionically conducting glasses and melts*Solid State Ion.* **105** 175
[193] Richert R 1998 Molecular dynamics analysed in terms of continuous measures of dynamic heterogeneity *J. Non-Cryst. Solids* **235–237** 41
[194] Cugliandolo L F and Iguain J L 2000 Hole-burning experiments within glassy models with infinite range interactions *Phys. Rev. Lett.* **85** 3448
[195] Cugliandolo L F and Iguain J L 2001 Reply to comment on 'Hole-burning experiments within glassy models with infinite range interactions' *Phys. Rev. Lett.* **87** 129603
[196] Chamberlin R V and Richert R 2001 Comment on 'Hole-burning experiments within glassy models with infinite range interactions' *Phys. Rev. Lett.* **87** 129601
[197] Diezemann G and Böhmer R 2001 Comment on 'Hole-burning experiments within glassy models with infinite range interactions' *Phys. Rev. Lett.* **87** 129602
[198] Reinsberg S A, Heuer A, Doliwa B, Zimmermann H and Spiess H W 2002 Comparative study of the NMR length scale of dynamic heterogeneities of three different glass formers *J. Non-Cryst. Solids*, at press
[199] Wang C-Y and Ediger M D 2000 Anomalous translational diffusion: a new constraint for models of molecular motion near the glass transition temperature *J. Phys. Chem.* B **104** 1724
[200] Qian J, Hentschke R and Heuer A 1999 On the origin of dynamic heterogeneities in glass-forming liquids *J. Chem. Phys.* **111** 10 177
[201] Zwanzig R 1990 Rate processes with dynamical disorder *Acc. Chem. Res.* **23** 148
[202] van Kampen N G 1992 *Stochastic Processes in Physics and Chemistry* (Amsterdam: North-Holland)
[203] Risken H 1989 *The Fokker–Planck Equation* (Berlin: Springer)
[204] Tracht U, Heuer A, Reinsberg S A and Spiess H W 1999 The rate memory of a polymer close to T_g as elucidated by reduced 4-D NMR echo experiments *Appl. Magn. Reson.* **17** 227